Sirindhorn International Institute of Technology
Thammasat University

Thesis CE-MS-2006-01

FLOW DEFORMATION COUPLED ANALYSIS USING FEM

Ahmed Faazal

FLOW DEFORMATION COUPLED ANALYSIS USING FEM

A Thesis Presented

by

Ahmed Faazal

Master of Science
Civil Engineering Program
Sirindhorn International Institute of Technology
Thammasat University
May 2007

FLOW DEFORMATION COUPLED ANALYSIS USING FEM

A Thesis Presented

by

Ahmed Faazal

Submitted to

Sirindhorn International Institute of Technology

Thammasat University

In partial fulfillment of the requirement for the degree of

MASTER OF SCIENCE IN ENGINEERING

Approved as to style and content by the Thesis Committee:

Chair and Advisor _____

Assoc. Prof. Krishna Murari Neaupane, D.Eng.

Member _____

Assoc. Prof. Pruettha Nanakorn, D.Eng.

Member _____

Asst. Prof. Napat Harnpornchai, Dr.Tech.

May 2007

Acknowledgements

First of all, the author would like to express his sincere gratitude to his advisor, Assoc. Prof. Krishna Murari Neaupane, for his invaluable guidance throughout the research. The author would also like to thank Assoc. Prof. Pruettha Nanakorn and Asst. Prof. Napat Harnpornchai for their valuable comments and suggestions throughout the research work and their willingness to be members of the thesis committee.

The author would also like to express his appreciation to Assoc. Prof. Noppadol Phienwej, Assoc. Dean, School of Civil Engineering & Technology, Asian Institute of Technology, for kindly accepting to be a thesis external examiner.

In addition, thoughtful thanks are extended to the secretaries of Civil Engineering Program, Ms. Chalida Yuenyaw and Ms. Supattra Manachitrungrueng, for their kind cooperation and services throughout this study.

Honest thanks are in order to the author's friends for their help and encouragement.

Last but not the least, sincere thanks are in order to the author's family for their moral support and invaluable advice.

Abstract

A coupled hydro-mechanical finite element analysis procedure for soil problems is presented which is both applicable for saturated and unsaturated soils. A detailed coupled formulation of the three governing equations has been presented using the Galerkin method.

As a model, a residual soil slope has been chosen, and analysed using the derived numerical code, DEFLOC (DEformation FLOw Coupled program), which has been developed in the MATLAB environment. The effects of hydraulic characteristics, matric suction and degree of saturation on the pore pressure and deformation behaviour of a residual soil slope under rainfall was investigated. The results reveal a typical process of infiltration into unsaturated soil slopes.

Table of Contents

List of Figures

List of Tables

Chapter 1

Introduction

1.1 General

The behavior of partially saturated soils can be very different to that of fully saturated or dry soils. For many geotechnical problems involving unsaturated soils, knowledge of the porewater pressures, the negative porewater pressure in particular, is of primary importance. The effect of negative porewater pressure (matric suction) on flow-deformation regime can not be overlooked where the concern is a shallow failure surface (Fredlund and Rahardjo, 1995).

Rainfall-triggered slope failures are the most common slope instability phenomenon in unsaturated residual soils along the monsoon affected areas of South Asia and South East Asia (Neaupane and Piantanakulchai, 2006; Singh et al., 2005). Such failures occur on both virgin and construction modified hillsopes on the northern and north eastern part of Thailand during rainy season. The hillslopes are generally covered with unsaturated residual soil and often shallow earth slips are predominant accounting for about 80 % of failures (ADPC, 2006). In general, the failures on unsaturated soil occur due to an increase in moisture content and a decrease in matric suction. Wetting reduces the additional shear strength provided by the matric suction to the failure (Krahn et al., 1989). A rise in the groundwater level also increases the unit weight and moisture content thereby reducing the resisting force and increasing the driving moment.

A fully coupled flow-deformation system is characterized by the procedure that rigorously incorporates the interactions among the three bulk phases of a deforming porous medium, and therefore, fluid flow and mechanical equilibrium equations are required to be solved simultaneously. In uncoupled analysis, however, a solution to the flow equation is first ought to determine the pore pressure changes in a given time step and pore pressure changes are then used as applied loads in a deformation analysis. The fluid flow and deformation analysis are carried out separately. The issue of coupling versus uncoupling in consolidation type problems has been previously addressed by several researchers (Biot and Willis 1957; Green and Wang 1990; Neaupane and Yamabe, 2001). As pointed out by Desai and Saxena 1997) and Lewis et al. (1989) coupling is generally accepted when the forcing function is applied to the displacement field e.g., by a physical load or a foundation. Hence, the response of unsaturated soils subjected to perturbations is described the coupling between fluid flow and deformation in this research.

Several attempts have been made to simulate multiphase flow in deforming porous media based on the theory of poroelasticity. However, only a few fully coupled models of multiphase flow in a deforming porous medium are available due to the complexities. Although the existing models are capable of reproducing some of the important features of the behavior of partially saturated soils, most models are basic, and impose limitations on the use of the equations and models because they do not usually consider down-slope

flows, rainfall intensity, and most importantly, the dependence of soil permeability on moisture content (Tsaparus, et al. 2002, Gasmo et al. 2000, Ng and Shi, 1989).

Early attempts to describe the behavior of partially saturated soils made the assumption that the effective stress principle is applicable to such soils and that the mechanical behavior can be fully described in the conventional (q, p') stress space. Generalized effective stress expressions were proposed to include partially saturated soils into the conventional soil mechanics framework, the best known being that proposed by Bishop (1959). The Bishop's approach proved capable of reproducing some features of the behavior of partially saturated soils, such as the shear strength increase due to suction, but could not explain others, such as wetting induced collapse. It is now generally accepted that two independent stress variables are necessary in order to explain the behavior of partially saturated soils. Bishop and Blight (1963) first used net total stress $(\sigma - p_a)$ and suction $(p_a - p_w)$ to investigate the volumetric and strength behavior of partially saturated soils and produced graphical representations of state surfaces and failure envelopes. Researchers suggest that any pair of stress state variables among the following: $(\sigma - p_a)$, $(\sigma - p_w)$ and $(p_a - p_w)$ can be adopted when describing partially saturated soil behavior. The most commonly used pair is net total stress $(\sigma - p_a)$ and suction $(p_a - p_w)$ (Alonso et al. 1999, 2000).

An analytical solution for a coupled problem in unsaturated soil is not possible without making several simplifying assumptions. Nevertheless, attempts have been made, in recent years, to come up with the closed form solution of the governing equations of unsaturated soils, including equilibrium equations and continuity flow equations (Gatmiri and Jabbari, 2005). Nevertheless, the numerical solution becomes indispensable for such a complex problem of investigating the behavior of partially saturated soils.

This research aims at developing a coupled hydro-mechanical numerical code, DEFLOC (DEformation FLOw Coupled program) and using the developed code to analyze the flow deformation behavior of an unsaturated soil subjected to rainfall infiltration. The finite element program was developed in the MATLAB environment and takes into account the basic features of unsaturated soil behavior.

1.2 Objectives and Scope of the Study

To perform a coupled finite element analysis of unsaturated soil problems, governing equations of inevitable importance are the mechanical equilibrium equations and the mass conservation equations, which have long been established. Using these governing equations, a finite element formulation can be carried out eliminating the use of deriving these equations in the first place. The objectives of this study are:

1) Carryout a finite element formulation on the governing equations.
2) Write a finite element code that can analyze a chosen physical problem.

The scope of this study is limited to:

1) Elastic behavior of the soil skeleton.
2) At the programming stage, pore air pressure is assumed to be a constant and equal to zero.

Chapter 2

Literature Review

2.1 Introduction

This chapter is subdivide into two parts. The first part explains the basic features of the mechanical behavior of partially saturated soils, particularly the volumetric and shear strength behavior of soils. The second part deals with the constitutive modeling of the mechanical behavior of the soils.

2.2 Mechanical behavior

2.2.1 Stress state variables and the effective stress principle

Previous models describing the behaviour of partially saturated soils made the assumption that the effective stress principle is applicable to such soils and that the mechanical behaviour can be fully described in the conventional (q, p') stress space. Generalised effective stress expressions were proposed in order to incorporate partially saturated soils into the conventional soil mechanics framework, the best known being that proposed by Bishop (1959):

$$\boldsymbol{\sigma}^{*} = \left(\boldsymbol{\sigma} - p_a\right) + \chi\left(p_a - p_w\right) \tag{2.1}$$

where χ is a function of the degree of saturation, p_a is the pore air pressure, and p_w is the pore water pressure. This approach proved capable of reproducing some of the features of partially saturated soils such as the shear strength increase due to suction but fails to give an explanation for some other features like wetting induced collapse. This was first demonstrated by Jennings & Burland (1962) who performed a series of oedometer, isotropic compression and wetting tests on partially saturated soils ranging from silty sands to silty clays. Their research showed that with the exception of the initially soaked samples, all the other air-dry samples collapsed upon wetting, which is in contrast to the effective stress principle according to which only swelling would be expected. Many preceding authors Burland (1965), Matyas & Radharkrishna (1968) and some others have also criticized the effective stress principle for partially saturated soils.

The collapse behaviour of partially saturates soils is due to an increase of the pore water pressure and is not unique to partially saturates soils only. Fully saturates soils may also collapse when the pore water pressure approaches the total stress resulting in a zero effective stress.

It is now generally accepted that in order to model the behaviour of partially saturates soils, two independent stress state variables are necessary. Bishop & Blight (1963) first used net stress (σ - p_a) and suction ($p_a - p_w$) to investigate the volumetric and

strength behavior of partially saturates soils and produced graphical representations of the state surfaces and failure envelopes for such soils as shown in Figure 2.1 and 2.2.

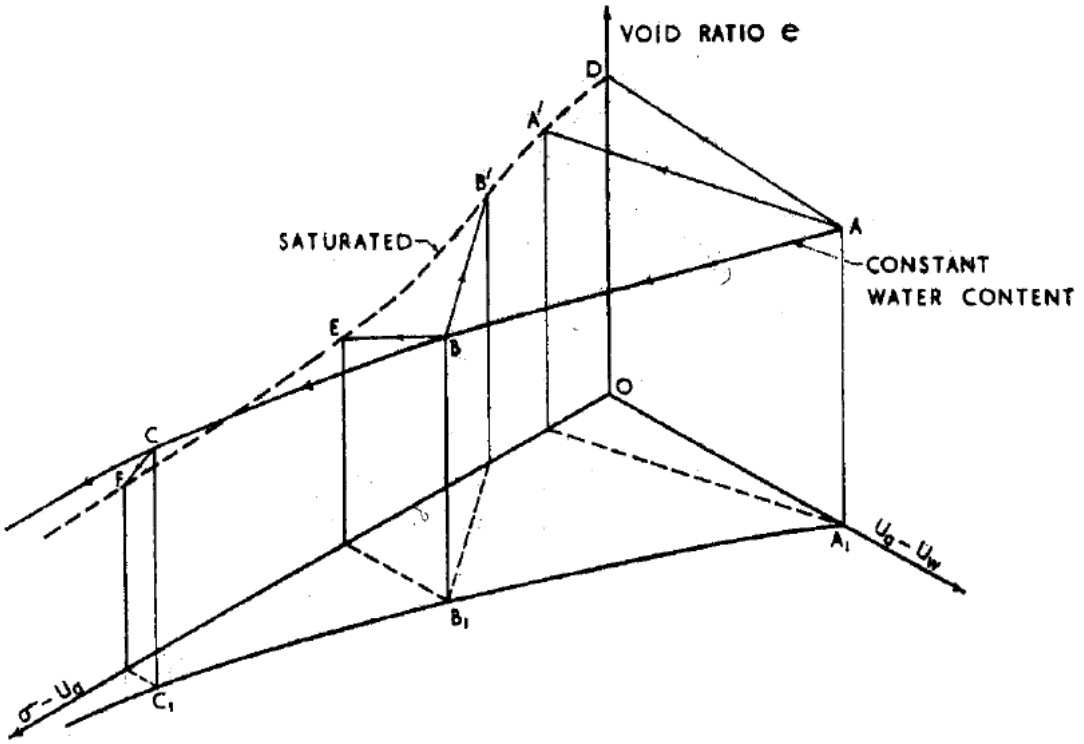

Figure 2.1: Void ratio state surface – Volume changes plotted in a void ratio-stress space

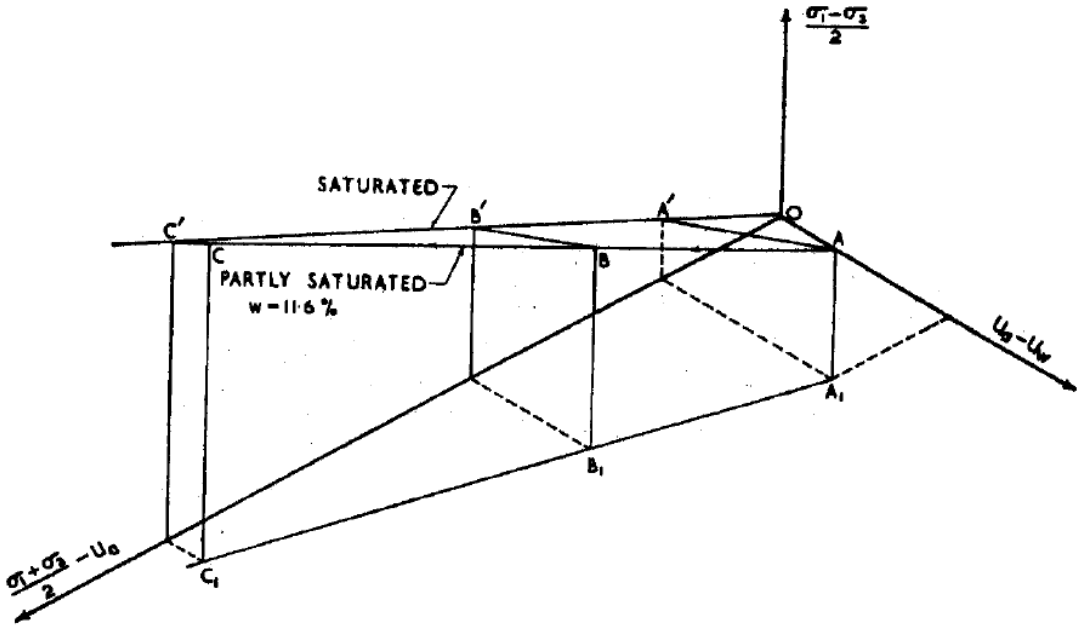

Figure 2.2: Results of tests on saturated and partially saturated clay

Fredlund & Mogenstern (1977) suggested that any pair of stress state variables among the following (σ - p_a), (σ - p_w) and suction ($p_a - p_w$) can be chosen to express the behaviour of

partially saturated soils. The most widely used pair is the net total stress (σ - p_a) and suction ($p_a - p_w$). Examples of some other stress state variables have been summarized in Table 2.1.

	Stress state variable 1	Stress state variable 1
Alonso et *al*. (1990) Cui et *al*. (1995) Wheeler & Sivakumar (1995)	(σ - p_a)	($p_a - p_w$)
Bolzon et *al*. (1996)	(σ - p_a) + $\chi(p_a - p_w)$	($p_a - p_w$)
Modaressi & Abou-Bekr (1994)	σ - π_c π_c = capillary pressure	π_c
Kohgo et *al*. (1993)	σ - p_{eq} p_{eq} = equivalent pore preusre	$p_a - p_w - s_e$ s_e = air entry suction

Table 2.1: Stress state variables used by some of the existing constitutive models

2.2.2 Volume change due to wetting and drying

The suction induced volumetric behavior of partially saturated soils at constant mean net stress can be explained as:

Volume changes due to drying

At the initial drying stages of saturated soil, the soil remains fully saturated and the total volume change is equal to the pore water volume change. At this stage the increase of suction is equal to the increase of total isotropic stress. The value of suction at which desaturation occurs is controlled by the soil type and varies significantly on the particle size for granular soils and on the pore size for clayey soils. The total volume changes can be expressed in terms of void ratio, e, and the water volume changes in terms of equivalent void ratio, e_w (= volume of water / volume of solids). The effects of suction changes are not equivalent to mean net stress changes once the soil has started to desaturate.

It is common practice to assume that for low plasticity soils, volumetric changes during drying beyond desaturation are small and reversible, but at high values of suction, plastic deformations may take place. Alonso et *al*. (1990) proposed that the yield suction point, s_0, beyond which the soil is elastoplastic, is independent to the confining stress and equal to the maximum previously attained value of suction. According to Wheeler & Karube (1996), yielding due to drying is only possible for partially saturated soils containing saturated clay packets. Chen et *al*. (1999) performed drying tests on compacted low plasticity loess which exhibited a distinct yield value of suction. The obtained yield suction results from his research were not in accordance with that proposed by Alonso et *al*. (1990). They later suggested that the value of the yield suction depends not only on the drying-wetting history but also on the initial soil density.

In the case of high plasticity expansive soils, the volumetric deformations due to increasing suction due to drying can be large and irreversible.

Volume changes due to wetting

One of the most distinctive features of partially saturated soils is the potential collapse behavior when subjected to wetting. Alonso et *al*. (1987) stated that a partially saturated soil may either expand or collapse upon wetting, depending on the confining stress. If the confining stress is sufficiently low, the soil will expand and collapse if the confining stress is sufficiently high. He also suggested that it is possible that a soil might experience a reversal in the volumetric behavior during wetting suggesting that the soil might initially expand followed by collapse. This behaviour has been reported amongst others by Escario & Saez (1973), Josa et *al*. (1987) and Burland & Ridley (1996). Figure 2.3 shows the initial swelling followed by collapse during wetting at constant load experienced by three samples of remoulded clay with different initial values of moisture content and tensile pore water pressure (Escario & Saez (1973)).

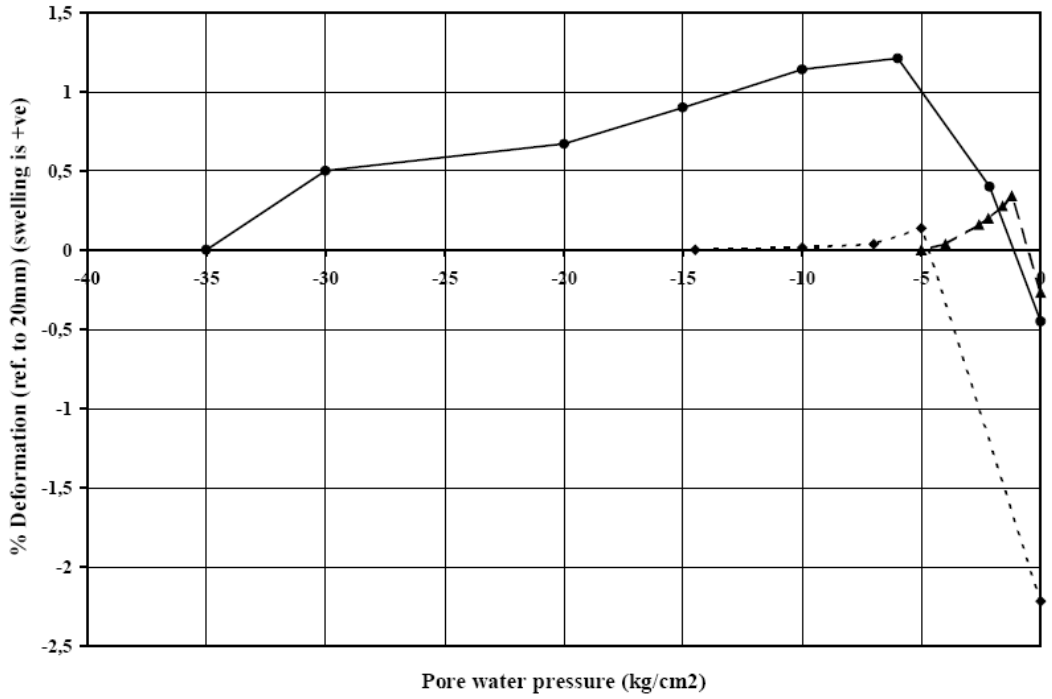

Figure 2.3: Swelling followed by collapse during wetting under constant load for three different initial values of tensile pore water pressure (after Escario & Saez (1973))

It can be summarized that in the case of low placity non-expansive soils, if the stress state is not high enough to cause collapse upon wetting, the swelling will be small and reversible. In the case of high plasticity expansive clays, the swelling will be large and irreversible. Experimental results from Matyas &Radharkrishna (1968), Booth (1975), Yudhbir (1982) and others indicate that for many soils the amount of collapse increases with confining stress at low stress regions, reaches a maximum and then decreases with stress becoming very small at high confining stresses.

2.2.3 Shear strength

At low values of suction, when the soil is still fully saturated, the shear strength is defined from the effective stresses and increases linearly with suction. Once the soil

becomes partially saturated, beyond the air entry value, the increase of shear strength with suction is smaller and non-linear.

Bishop, Alpan, Blight & Donald (1960) extended the Mohr-Coulomb failure criterion to partially saturated soil conditions through the use of Bishop's effective stress expression. They proposed the following expression for the shear strength of soils (which is both applicable for saturated and partially saturated soils):

$$\tau = c' + (\sigma - p_a)\tan\phi' + \chi(p_a - p_w)\tan\phi' \qquad (2.2)$$

where τ is the shear strength of the soil, c' is the effective cohesion, ϕ' is the angle of shearing resistance and χ is the effective stress parameter, which varies between 0 and 1, where 0 being the value for the fully saturated case, and 1 being the value for the case where the soil is completely dry. Fredlund, Morgenstern & Widger (1978) proposed a modified version of expression (2.2):

$$\tau = c' + (\sigma - p_a)\tan\phi' + (p_a - p_w)\tan\phi^b \qquad (2.3)$$

where ϕ^b is the slope of the failure surface in the τ - s plane. It was concluded that both ϕ' and ϕ^b are independent of suction, and hence the effect of suction on the shear strength is equivalent to an increase of the effective cohesion:

$$c = c' + (p_a - p_w)\tan\phi^b \qquad (2.4)$$

Equation (2.4) reduces to the fully saturated Mohr Coulomb failure criterion when suction is equal to zero. Experimental results from Escario & Juca (1989), Gan & Fredlund (1996) and Nishimura & Toyota (2002) shows that at high values of suction, ϕ^b becomes negative implying that at very high suctions as the soil becomes completely dry the increase of apparent cohesion due to suction tends to zero.

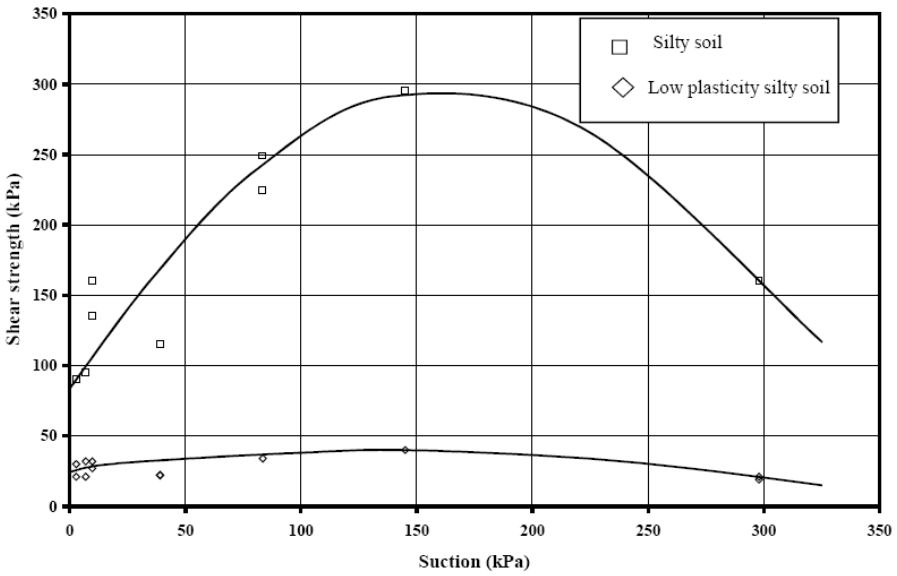

Figure 2.4: Changes in shear strength with soil suction (data from Nishimura & Toyota (2002)

2.3 Constitutive models for partially saturated soils

Constitutive models for partially saturated soils can be broadly divided into two categories, namely, elastic models and elastoplastic models.

Elastic models relate strain increments to increments of net stress and suction. Such models have been proposed by Fredlund & Morgenstern (1976) and Lloret et al. (1987). Wheeler & Karube (1996) in the state of the art report on constitutive modelling presented a comprehensive review of the models of this type. They stated that although elastic models have the advantage that it is relatively easy to implement them within numerical analysis and measure the relevant parameters, there are major disadvantages. The most important is that there is no distinction between reversible and irreversible strains, which means that they can only be used in problems that involve only monotonic loading and unloading. Even in this case there are a number of weaknesses. Consequently, elastic models are not considered with in this thesis and will not be mentioned further.

One of the first elastoplastic constitutive models to be developed for partially saturated soils was the Barcelona Basic Model (Alonso et al. (1990)), which was based on the theoretical framework proposed by Alonso et al. (1987). This model was an extension of the Modified Cam-Clay model for fully saturated soils to partially saturated states through the introduction of the concept of the Loading-Collapse yield surface (Fig.2-26). The concept allows the reproduction of many important features of partially saturated soil behavior, such as collapse upon wetting, and is the basis upon which most other elastoplastic models have been developed.

Chapter 3

Mathematical Formulation

3.1 Introduction to Finite Element Analysis

A number of methods of analysis exist in geotechnical engineering. These fall into three broad categories; closed form, simple (e.g. limit equilibrium, stress field, limit analysis) and numerical (beam-spring and full numerical) analysis. In order to obtain an exact theoretical solution the requirements of equilibrium, compatibility, material behavior and boundary conditions must all be satisfied. While all the methods have their respective advantages and disadvantages, only full numerical analysis satisfies all the required conditions and is therefore capable of approximating sufficiently the exact solution to complex geotechnical problems.

One of the most widely used methods of full numerical analysis is the finite element method. The first step in a Finite Element analysis is to define and quantify the geometry of the boundary value problem under investigation. This is then replaced by an equivalent finite element mesh, which consists of small regions called finite elements. Finite elements are usually triangular or quadrilateral in shape, for two-dimensional problems, and their geometry is specified in terms of the coordinates of key points called nodes. The nodes in the simplest case are located at the corners of the element.

3.2 Approximation of primary unknown variables

The primary unknown variables for partially saturated soil problems are the displacements, pore water pressure and pore air pressure which varies over the problem domain. Stresses, strains, degree of saturation, permeability, porosity, and volumetric water content are all treated as secondary variables, which can be expressed in terms of the primary variables. In two-dimensional plane strain analyses the displacement field is characterized by the two global displacements u and v, in the x and y coordinate directions respectively. An assumption needs to be made about the form of the variation of the primary variables over the domain under investigation. The accuracy of a finite element analysis depends on the size of the elements and the nature of the approximation.

The element type chosen is 4 node quadrilateral elements, which conforms to C^1 continuity.

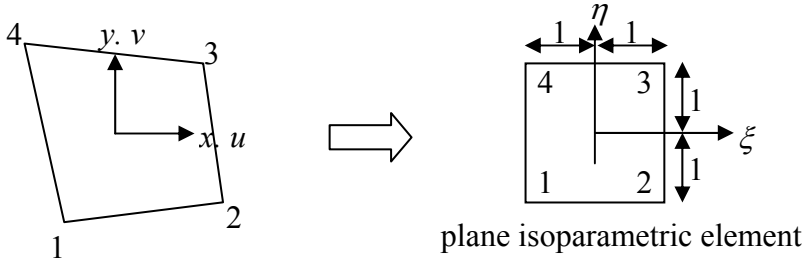

Figure 3.1: 4 node – plane isoparametric element in xy and $\xi\eta$ space

This type of elements provides interelement continuity of the field quantity ϕ and its first derivatives at nodes, but not interelement continuity of all second derivatives of ϕ.
Axes ξ and η pass though the midpoints of opposite sides and the sides of the element are at $\xi = \pm 1$ and $\eta = \pm 1$.

A point in ξ-η space can be mapped into x-y space by using:

$$x = \sum_{i=1}^{4} N_i x_i \quad ; \quad y = \sum_{i=1}^{4} N_i y_i \tag{2.2.1}$$

where x_i and y_i are the coordinate values of i^{th} node.

Individual shape functions can be expressed as:

$$\begin{aligned} N_1 &= \frac{1}{4}(1-\xi)(1-\eta) \\ N_2 &= \frac{1}{4}(1+\xi)(1-\eta) \\ N_3 &= \frac{1}{4}(1+\xi)(1+\eta) \\ N_4 &= \frac{1}{4}(1-\xi)(1+\eta) \end{aligned} \tag{2.2.2}$$

Where derivatives of [**N**] with respect to the global coordinates (x, y) are required, derivatives can be converted from one coordinate system to the other by using the chain rule of partial differentiation, which can be written in matrix form for the two dimensional case as:

$$\begin{Bmatrix} \frac{\partial}{\partial \xi} \\ \frac{\partial}{\partial \eta} \end{Bmatrix} = \begin{bmatrix} \frac{\partial x}{\partial \xi} & \frac{\partial y}{\partial \xi} \\ \frac{\partial x}{\partial \eta} & \frac{\partial y}{\partial \eta} \end{bmatrix} \begin{Bmatrix} \frac{\partial}{\partial x} \\ \frac{\partial}{\partial y} \end{Bmatrix} = [\mathbf{J}] \begin{Bmatrix} \frac{\partial}{\partial x} \\ \frac{\partial}{\partial y} \end{Bmatrix} \tag{2.2.3}$$

or

$$\begin{Bmatrix} \frac{\partial}{\partial x} \\ \frac{\partial}{\partial y} \end{Bmatrix} = [\mathbf{J}]^{-1} \begin{Bmatrix} \frac{\partial}{\partial \xi} \\ \frac{\partial}{\partial \eta} \end{Bmatrix} \quad \text{i.e.} \quad \begin{Bmatrix} \frac{\partial N_i}{\partial x} \\ \frac{\partial N_i}{\partial y} \end{Bmatrix} = [\mathbf{J}]^{-1} \begin{Bmatrix} \frac{\partial N_i}{\partial \xi} \\ \frac{\partial N_i}{\partial \eta} \end{Bmatrix} \tag{2.2.4}$$

where [**J**] is the Jacobian matrix:

$$[\mathbf{J}] = \begin{bmatrix} J_{11} & J_{12} \\ J_{21} & J_{22} \end{bmatrix} = \begin{bmatrix} \dfrac{\partial x}{\partial \xi} & \dfrac{\partial y}{\partial \xi} \\ \dfrac{\partial x}{\partial \eta} & \dfrac{\partial y}{\partial \eta} \end{bmatrix} \tag{2.2.5}$$

For example, J_{11} can be calculated as

$$\begin{aligned} J_{11} &= \frac{\partial x}{\partial \xi} = \sum_{i=1}^{4} \frac{\partial N_i(\xi,\eta)}{\partial \xi} x_i \\ &= -\frac{1}{4}(1-\eta)x_1 + \frac{1}{4}(1-\eta)x_2 + \frac{1}{4}(1+\eta)x_3 - \frac{1}{4}(1+\eta)x_4 \end{aligned}$$

The determinant of the Jacobian matrix is of special interest as it is used in the transformation of the integrals as:

$$\iint (...)\,\mathrm{d}x\ \mathrm{d}y = \int_{-1}^{1}\int_{-1}^{1} (...)\det|\mathbf{J}|\ \mathrm{d}\xi\mathrm{d}\eta \tag{2.2.6}$$

where $\det|\mathbf{J}|$ is the determinant of Jacobian matrix, also known as "The Jacobian".

3.3 Formulation of water mass balance equation

The water mass balance equation for unsaturated soil is:

$$\frac{\partial(\rho_w n S_r)}{\partial t} + \mathrm{div}(\rho_w \mathbf{v}_\mathrm{w}) = 0 \tag{2.3.1}$$

where ρ_w is the density of water, n is porosity, S_r is the degree of saturation and $\mathbf{v_w}$ is the velocity of water.

Density of water is assumed to be constant and hence (2.3.1) can be expressed as:

$$\frac{\partial}{\partial t}(n S_r) + \mathrm{div}(\mathbf{v}_\mathrm{w}) = 0 \tag{2.3.2}$$

The arbitrary weight function ϕ, in accordance with the Galerkin method is given by:

$$\phi = \mathbf{N}_\mathrm{n}\bar{\boldsymbol{\varphi}} \tag{2.3.3}$$

where,

$$\mathbf{N}_{\mathrm{n}} = \begin{bmatrix} N_1 & N_2 & N_3 & N_4 \end{bmatrix}, \tag{2.3.4}$$

$$\bar{\boldsymbol{\varphi}} = \begin{bmatrix} \phi_1 & \phi_2 & \phi_3 & \phi_4 \end{bmatrix}^{\mathrm{T}} \tag{2.3.5}$$

Multiplying (2.3.2) by (2.3.3) and taking arbitrary volume integral of the result (limiting the scope for two-dimensional problems and considering constant element thickness) gives

$$\int_A \phi \left[\frac{\partial}{\partial t}\left(nS_r\right) + \operatorname{div}\left(\mathbf{v}_{\mathrm{w}}\right) \right] dA = 0 \tag{2.3.6}$$

where,

$$\mathbf{v}_{\mathrm{w}} = \begin{bmatrix} v_{wx} \\ v_{wy} \end{bmatrix} \tag{2.3.7}$$

Equation (2.3.6) can be simplified further to give:

$$\int_A \phi \frac{\partial}{\partial t}\left(nS_r\right)\, dA + \int_A \phi\, \operatorname{div}\left(\mathbf{v}_{\mathrm{w}}\right) dA = 0 \tag{2.3.8}$$

Using Gauss Theorem, the second term from left hand side of (2.3.8) can be written as:

$$\int_A \phi\, \operatorname{div}\left(\mathbf{v}_{\mathbf{w}}\right)\, dA = \oint_\Gamma \phi\, \mathbf{v}_{\mathbf{w}}^{\mathbf{T}}\mathbf{n}\, d\Gamma - \int_A \left(\nabla\phi\right)^{\mathrm{T}} \mathbf{v}_{\mathrm{w}}\, dA \tag{2.3.9}$$

where **n** is the unit vector normal to the boundary and directed outwards. For the two dimensional case, **n** can be written as:

$$\mathbf{n} = \begin{bmatrix} n_x \\ n_y \end{bmatrix} \tag{2.3.10}$$

Substituting (2.3.9) into (2.3.8):

$$\int_A \phi \frac{\partial}{\partial t}\left(nS_r\right)\, dA + \oint_\Gamma \phi\, \mathbf{v}_{\mathbf{w}}^{\mathbf{T}}\mathbf{n}\, d\Gamma - \int_A \left(\nabla\phi\right)^{\mathrm{T}} \mathbf{v}_{\mathrm{w}}\, dA = 0 \tag{2.3.11}$$

Since ϕ is arbitrary, the matrix φ is arbitrary. So we can conclude:

$$\nabla\phi = \left(\nabla \mathbf{N}_{\mathbf{n}}\right)\bar{\boldsymbol{\varphi}} = \mathbf{B}_{\mathbf{n}}\bar{\boldsymbol{\varphi}} \tag{2.3.12}$$

where

$$\mathbf{B_n} = \begin{bmatrix} \frac{\partial}{\partial x} N_1 & \frac{\partial}{\partial x} N_2 & \frac{\partial}{\partial x} N_3 & \frac{\partial}{\partial x} N_4 \\ \frac{\partial}{\partial y} N_1 & \frac{\partial}{\partial y} N_2 & \frac{\partial}{\partial y} N_3 & \frac{\partial}{\partial y} N_4 \end{bmatrix} \tag{2.3.13}$$

Also, as:

$$\phi = \phi^{\mathrm{T}}, \ \phi = \bar{\boldsymbol{\varphi}}^{\mathbf{T}} \mathbf{N}_{\mathbf{n}}^{\mathbf{T}} \tag{2.3.14}$$

Using (2.3.3), (2.3.12), (2.3.14) and using the fact that $\boldsymbol{\varphi}$ is independent of position, (2.3.11) can be simplified and written as:

$$\bar{\boldsymbol{\varphi}}^{\mathbf{T}} \left[\int_A \mathbf{N}_{\mathbf{n}}^{\mathbf{T}} \frac{\partial}{\partial t} \left(n S_r \right) \, dA + \oint_{\boldsymbol{\Gamma}} \mathbf{N}_{\mathbf{n}}^{\mathbf{T}} \mathbf{v}_{\mathbf{w}}^{\mathbf{T}} \mathbf{n} \, d\boldsymbol{\Gamma} - \int_A \mathbf{B}_{\mathbf{n}}^{\mathbf{T}} \mathbf{v}_{\mathrm{w}} \, dA \right] = 0 \tag{2.3.15}$$

As (2.3.15) should hold for arbitrary $\bar{\boldsymbol{\varphi}}^{\mathbf{T}}$ matrices, it can be concluded that:

$$\int_A \mathbf{N}_{\mathbf{n}}^{\mathbf{T}} \frac{\partial}{\partial t} \left(n S_r \right) \, dA + \oint_{\boldsymbol{\Gamma}} \mathbf{N}_{\mathbf{n}}^{\mathbf{T}} \mathbf{v}_{\mathbf{w}}^{\mathbf{T}} \mathbf{n} \, d\boldsymbol{\Gamma} - \int_A \mathbf{B}_{\mathbf{n}}^{\mathbf{T}} \mathbf{v}_{\mathrm{w}} \, dA = 0 \tag{2.3.16}$$

Now introducing the term q_w, which is the water flux across the boundary, (2.3.16) becomes:

$$\int_A \mathbf{N}_{\mathbf{n}}^{\mathbf{T}} \frac{\partial}{\partial t} \left(n S_r \right) \, dA + \oint_{\boldsymbol{\Gamma}} \mathbf{N}_{\mathbf{n}}^{\mathbf{T}} q_w \, d\boldsymbol{\Gamma} - \int_A \mathbf{B}_{\mathbf{n}}^{\mathbf{T}} \mathbf{v}_{\mathrm{w}} \, dA = 0 \tag{2.3.17}$$

where,

$$q_w = \mathbf{v}_{\mathbf{w}}^{\mathbf{T}} \mathbf{n} \tag{2.3.18}$$

Water flow is described by a generalization of Darcy's law which can be expressed as:

$$\mathbf{v}_{\mathrm{w}} = -K_w \nabla \left(p_w / \gamma_w + z \right) \tag{2.3.19}$$

where $\mathbf{K}_{\mathrm{w}}$ is the coefficient of permeability, z the elevation head and γ_w the specific weight of water (assumed constant).

Equation (2.3.19) can be simplified and written as:

$$\mathbf{v}_{\mathrm{w}} = -K_w \left(\frac{1}{\gamma_w} \nabla p_w + \nabla z \right) \tag{2.3.20}$$

where,

$$\nabla p_w = \begin{bmatrix} \dfrac{\partial}{\partial x} \\ \dfrac{\partial}{\partial y} \end{bmatrix} p_w = \begin{bmatrix} \dfrac{\partial p_w}{\partial x} \\ \dfrac{\partial p_w}{\partial y} \end{bmatrix} \tag{2.3.21}$$

Jacquard (1988) proposed a relationship for coefficient of permeability, K_w interms of suction as

$$K_w = \frac{A_w K_{ws}}{A_w + \left(C_w \left(p_a - p_w\right)\right)^{B_w}} \tag{2.3.22}$$

where A_w, B_w, C_w and K_{ws} are constants.

Substituting (2.3.20) into (2.3.17):

$$\int_A \mathbf{N}_\mathbf{n}^\mathrm{T} \frac{\partial}{\partial t}\left(nS_r\right)\, dA + \oint_{\boldsymbol{\Gamma}} \mathbf{N}_\mathbf{n}^\mathrm{T} q_w \, d\boldsymbol{\Gamma} + \int_A \mathbf{B}_\mathbf{n}^\mathrm{T} K_w \left(\frac{1}{\gamma_w}\nabla p_w + \nabla z\right) dA = 0 \tag{2.3.23}$$

Using Trial Function Approximation and discretizing for pressure of water,

$$\int_A \mathbf{N}_\mathbf{n}^\mathrm{T} \frac{\partial}{\partial t}\left(nS_r\right)\, dA + \oint_{\boldsymbol{\Gamma}} \mathbf{N}_\mathbf{n}^\mathrm{T} q_w \, d\boldsymbol{\Gamma} + \int_A \mathbf{B}_\mathbf{n}^\mathrm{T} K_w \left(\frac{1}{\gamma_w}\nabla\left(\mathbf{N}_\mathrm{n}\overline{\mathbf{p}_\mathrm{w}}\right) + \nabla z\right) dA = 0 \tag{2.3.24}$$

where,

$$\overline{\mathbf{p}_\mathrm{a}} = \begin{bmatrix} p_{a_1} & p_{a_2} & p_{a_3} & p_{a_4} \end{bmatrix}^\mathrm{T}, \tag{2.3.25}$$

$$\overline{\mathbf{p}_\mathrm{w}} = \begin{bmatrix} p_{w_1} & p_{w_2} & p_{w_3} & p_{w_4} \end{bmatrix}^\mathrm{T} \tag{2.3.26}$$

Simplifying the third term from L.H.S. of (2.3.24), equation (2.3.24) can be rewritten as:

$$\begin{aligned} &\int_A \mathbf{N}_\mathbf{n}^\mathrm{T} \frac{\partial}{\partial t}\left(nS_r\right)\, dA + \oint_{\boldsymbol{\Gamma}} \mathbf{N}_\mathbf{n}^\mathrm{T} q_w \, d\boldsymbol{\Gamma} + \int_A \frac{1}{\gamma_w}\mathbf{B}_\mathbf{n}^\mathrm{T} K_w \nabla\left(\mathbf{N}_\mathrm{n}\overline{\mathbf{p}_\mathrm{w}}\right) dA \\ &+ \int_A \mathbf{B}_\mathbf{n}^\mathrm{T} K_w \nabla z \, dA = 0 \end{aligned} \tag{2.3.27}$$

Further simplification of the third term from L.H.S. of (2.3.27):

$$\begin{aligned} &\int_A \mathbf{N}_\mathbf{n}^\mathrm{T} \frac{\partial}{\partial t}\left(nS_r\right)\, dA + \oint_{\boldsymbol{\Gamma}} \mathbf{N}_\mathbf{n}^\mathrm{T} q_w \, d\boldsymbol{\Gamma} + \int_A \frac{1}{\gamma_w}\mathbf{B}_\mathbf{n}^\mathrm{T} K_w \nabla \mathbf{N}_\mathrm{n}\overline{\mathbf{p}_\mathrm{w}} \, dA \\ &+ \int_A \mathbf{B}_\mathbf{n}^\mathrm{T} K_w \nabla z \, dA = 0 \end{aligned} \tag{2.3.28}$$

The partial derivative of porosity with respect to time maybe written as

$$\frac{\partial}{\partial t} n \;=\; \mathbf{m}^{\mathbf{T}} \frac{\partial}{\partial t} \boldsymbol{\varepsilon} \;=\; \mathbf{m}^{\mathbf{T}} \frac{\partial}{\partial t} \widetilde{\nabla} \mathbf{u} \tag{2.3.29}$$

where

$$\mathbf{m}^{\mathbf{T}} = \begin{bmatrix} 1 & 1 & 0 \end{bmatrix} \tag{2.3.30}$$

For unsaturated soils, degree of saturation varies strongly with matric suction and hence the relationship proposed by Bourgeois (1986) is chosen, which is expressed as

$$S_r = S_{ri} + \frac{A_w \left(S_{rs} - S_{ri} \right)}{A_w + \left(C_w \left(p_a - p_w \right) \right)^{B_w}} \tag{2.3.31}$$

where A_w, B_w, C_w, S_{ri} and S_{rs} constants (Van Genuchten 1980, Bourgeois 1986).

In soil problems, an increase in suction is accompanied by a decrease in the degree of saturation and decrease in suction results in an increase in the degree of saturation, ultimately approaching to one (saturated condition).

Using the chain rule of differentiation,

$$\frac{\partial S_r}{\partial t} = \frac{\partial S_r}{\partial p_w} \times \frac{\partial p_w}{\partial t} \tag{2.3.32}$$

Using (2.3.29) and (2.3.32), $\frac{\partial}{\partial t}\left(n S_r \right)$ can be simplified as

$$\begin{aligned} \frac{\partial}{\partial t}\left(n S_r \right) &= n \frac{\partial}{\partial t}\left(S_r \right) + S_r \frac{\partial}{\partial t}\left(n \right) \\ &= \left[n \; \frac{\partial S_r}{\partial p_w} \frac{\partial p_w}{\partial t} \right] + \left[S_r \frac{\partial}{\partial t}\left(\mathbf{m}^{\mathbf{T}} \widetilde{\nabla} \mathbf{u} \right) \right] \end{aligned} \tag{2.3.33}$$

Discretizing for pressure of air, pressure of water and from (2.4.42),

$$\frac{\partial}{\partial t}\left(n S_r \right) = \left[n \frac{\partial S_r}{\partial p_w} \mathbf{N_n} \frac{\partial}{\partial t} \overline{\mathbf{p_w}} \right] + \left[S_r \frac{\partial}{\partial t}\left(\mathbf{m}^{\mathbf{T}} \mathbf{B_m} \bar{\mathbf{u}} \right) \right] \tag{2.3.34}$$

Simplifying (2.3.34) further

$$\frac{\partial}{\partial t}\left(n S_r \right) = \left[n \frac{\partial S_r}{\partial p_w} \mathbf{N_n} \frac{\partial}{\partial t} \overline{\mathbf{p_w}} \right] + \left[S_r \mathbf{m}^{\mathbf{T}} \mathbf{B_m} \frac{\partial}{\partial t}\left(\bar{\mathbf{u}} \right) \right] \tag{2.3.35}$$

Now, the first term from left hand side of (2.3.28) can be simplified as

$$\int_A \mathbf{N}_\mathbf{n}^\mathrm{T} \frac{\partial}{\partial t}\left(nS_r\right)\, dA = \int_A \mathbf{N}_\mathbf{n}^\mathrm{T} n \frac{\partial S_r}{\partial p_w} \mathbf{N}_\mathbf{n} \frac{\partial}{\partial t}\overline{\mathbf{p}_\mathbf{w}}\, dA + \int_A \mathbf{N}_\mathbf{n}^\mathrm{T} S_r \mathbf{m}^\mathrm{T} \mathbf{B}_\mathbf{m} \frac{\partial}{\partial t}\left(\overline{\mathbf{u}}\right)\, dA \quad (2.3.36)$$

The water mass balance equation can be now written as

$$\begin{aligned} &\int_A \mathbf{N}_\mathbf{n}^\mathrm{T} n \frac{\partial S_r}{\partial p_w} \mathbf{N}_\mathbf{n} \frac{\partial}{\partial t}\overline{\mathbf{p}_\mathbf{w}}\, dA + \int_A \mathbf{N}_\mathbf{n}^\mathrm{T} S_r \mathbf{m}^\mathrm{T} \mathbf{B}_\mathbf{m} \frac{\partial}{\partial t}\left(\overline{\mathbf{u}}\right)\, dA \\ &+\oint_\Gamma \mathbf{N}_\mathbf{n}^\mathrm{T} q_w\, d\boldsymbol{\Gamma} + \int_A \frac{1}{\gamma_w} \mathbf{B}_\mathbf{n}^\mathrm{T} K_w \nabla \mathbf{N}_\mathrm{n} \overline{\mathbf{p}_\mathrm{w}}\, dA + \int_A \mathbf{B}_\mathbf{n}^\mathrm{T} K_w \nabla z\, dA = 0 \end{aligned} \quad (2.3.37)$$

Equation (2.3.37) can be rewritten as

$$\begin{aligned} &\int_A \mathbf{N}_\mathbf{n}^\mathrm{T} n \frac{\partial S_r}{\partial p_w} \mathbf{N}_\mathbf{n}\, dA\ \frac{\partial}{\partial t}\overline{\mathbf{p}_\mathbf{w}} \\ &+\int_A \mathbf{N}_\mathbf{n}^\mathrm{T} S_r \mathbf{m}^\mathrm{T} \mathbf{B}_\mathbf{m}\, dA\ \frac{\partial}{\partial t}\left(\overline{\mathbf{u}}\right) \\ &+\oint_\Gamma \mathbf{N}_\mathbf{n}^\mathrm{T} q_w\, d\boldsymbol{\Gamma} + \int_A \frac{1}{\gamma_w} \mathbf{B}_\mathbf{n}^\mathrm{T} K_w \mathbf{B}_\mathrm{n} \overline{\mathbf{p}_\mathrm{w}}\, dA + \int_A \mathbf{B}_\mathbf{n}^\mathrm{T} K_w \nabla z\, dA = 0 \end{aligned} \quad (2.3.38)$$

Equation (2.3.38) can be more concisely written as

$$\mathbf{C}_\mathbf{1}^\mathbf{1} \frac{\partial}{\partial t}\left(\overline{\mathbf{p}_\mathbf{w}}\right) + \mathbf{C}_\mathbf{1}^\mathbf{2} \frac{\partial}{\partial t}\left(\overline{\mathbf{u}}\right) + \mathbf{C}_\mathbf{1}^\mathbf{3} + \mathbf{C}_\mathbf{1}^\mathbf{4} \overline{\mathbf{p}_\mathrm{w}} + \mathbf{C}_\mathbf{1}^\mathbf{5} = 0 \quad (2.3.39)$$

where

$$\begin{aligned} \mathbf{C}_\mathbf{1}^\mathbf{1} &= \int_A \mathbf{N}_\mathbf{n}^\mathrm{T} n \frac{\partial S_r}{\partial p_w} \mathbf{N}_\mathbf{n}\, dA \\ \mathbf{C}_\mathbf{1}^\mathbf{2} &= \int_A \mathbf{N}_\mathbf{n}^\mathrm{T} S_r \mathbf{m}^\mathrm{T} \mathbf{B}_\mathbf{m}\, dA \\ \mathbf{C}_\mathbf{1}^\mathbf{3} &= \oint_\Gamma \mathbf{N}_\mathbf{n}^\mathrm{T} q_w\, d\boldsymbol{\Gamma} \\ \mathbf{C}_\mathbf{1}^\mathbf{4} &= \int_A \frac{1}{\gamma_w} \mathbf{B}_\mathbf{n}^\mathrm{T} K_w \mathbf{B}_\mathrm{n}\, dA \\ \mathbf{C}_\mathbf{1}^\mathbf{5} &= \int_A \mathbf{B}_\mathbf{n}^\mathrm{T} K_w \nabla z\, dA \end{aligned} \quad (2.3.40)$$

3.4 Formulation of mechanical equilibrium equation

The general momentum balance equation can be written as:

$$\tilde{\nabla}^{\mathbf{T}}\boldsymbol{\sigma} + \mathbf{b} = 0 \tag{2.4.1}$$

where,

$$\tilde{\nabla}^{\mathbf{T}} = \begin{bmatrix} \frac{\partial}{\partial x} & 0 & \frac{\partial}{\partial y} \\ 0 & \frac{\partial}{\partial y} & \frac{\partial}{\partial x} \end{bmatrix}, \quad \boldsymbol{\sigma} = \begin{bmatrix} \sigma_{\mathrm{x}} \\ \sigma_{\mathrm{y}} \\ \sigma_{\mathrm{xy}} \end{bmatrix}, \quad \mathbf{b} = \begin{bmatrix} b_{\mathrm{x}} \\ b_{\mathrm{y}} \end{bmatrix} \tag{2.4.2}$$

where $\boldsymbol{\sigma}$ is the total stress, ρ the soil density and **b** the body forces.

For this particular problem these body forces are due to gravity and they act in the negative direction of the y-axis. i.e.

$$\mathbf{b} = \begin{bmatrix} 0 \\ -\rho g \end{bmatrix} \tag{2.4.3}$$

If air density is assumed to be negligible, soil density ρ can be written interms of the densities of soil and water phases as:

$$\rho = (1-n)\rho_s + nS_r\rho_w \tag{2.4.4}$$

where ρ is the soil density, ρ_s the density of solid phase, ρ_w the density of water and n is the soil porosity.

Carrying out the matrix multiplications of Eq. (2.4.1) gives

$$\begin{aligned} \frac{\partial \sigma_x}{\partial x} + \frac{\partial \sigma_{xy}}{\partial y} + b_x = 0 \\ \frac{\partial \sigma_y}{\partial y} + \frac{\partial \sigma_{xy}}{\partial x} + b_y = 0 \end{aligned} \tag{2.4.5}$$

On the boundary of the body, the traction vector **t** has components

$$\mathbf{t} = \begin{bmatrix} t_x \\ t_y \end{bmatrix} \tag{2.4.6}$$

This traction vector must fulfill the boundary conditions, i.e.

$$\begin{aligned} t_x = \sigma_x n_x + \sigma_{xy} n_y \\ t_y = \sigma_{xy} n_x + \sigma_y n_y \end{aligned} \tag{2.4.7}$$

Consider the arbitrary vector $\boldsymbol{\omega}$

$$\boldsymbol{\omega} = \begin{bmatrix} \omega_x \\ \omega_y \end{bmatrix} \tag{2.4.8}$$

So,

$$\left(\tilde{\nabla}\boldsymbol{\omega}\right)^{\mathrm{T}} \boldsymbol{\sigma} = \frac{\partial \omega_x}{\partial x}\sigma_x + \frac{\partial \omega_y}{\partial y}\sigma_y + \left(\frac{\partial \omega_x}{\partial y} + \frac{\partial \omega_y}{\partial x}\right)\sigma_{xy} \tag{2.4.9}$$

Multiply the first Equation of (2.4.5) by the arbitrary function ω_x and integrate over the volume V to obtain

$$\int_V \omega_x \frac{\partial \sigma_x}{\partial x}\, dV + \int_V \omega_x \frac{\partial \sigma_{xy}}{\partial y}\, dV + \int_V \omega_x b_x\, dV = 0 \tag{2.4.10}$$

By performing integration by parts on Eq. (2.4.10) using the Green-Gauss theorem given in the form

$$\begin{aligned} \int_V \phi \frac{\partial \psi}{\partial x}\, dV &= \int_S \phi\psi n_x\, dS - \int_V \frac{\partial \phi}{\partial x}\psi\, dV \\ \int_V \phi \frac{\partial \psi}{\partial y}\, dV &= \int_S \phi\psi n_y\, dS - \int_V \frac{\partial \phi}{\partial y}\psi\, dV \end{aligned} \tag{2.4.11}$$

the result becomes

$$\int_S \omega_x \sigma_x n_x\, dS - \int_V \frac{\partial \omega_x}{\partial x}\sigma_x\, dV + \int_S \omega_x \sigma_{xy} n_y\, dS - \int_V \frac{\partial \omega_x}{\partial y}\sigma_{xy}\, dV + \int_V \omega_x b_x\, dV = 0 \tag{2.4.12}$$

The component t_x of the traction vector $\mathbf{t}$ is given by (2.4.7), i.e. the expression above reduces to

$$\int_S \omega_x t_x\, dS - \int_V \left(\frac{\partial \omega_x}{\partial x}\sigma_x + \frac{\partial \omega_x}{\partial y}\sigma_{xy}\right) dV + \int_V \omega_x b_x\, dV = 0 \tag{2.4.13}$$

In a similar manner, the second term of (2.4.5) can be manipulated to yield

$$\int_S \omega_y t_y\, dS - \int_V \left(\frac{\partial \omega_y}{\partial x}\sigma_{xy} + \frac{\partial \omega_y}{\partial y}\sigma_y\right) dV + \int_V \omega_y b_y\, dV = 0 \tag{2.4.14}$$

Addition of Eqs. (2.4.13) & (2.4.14) gives

$$\begin{aligned}&\int_S \left(\omega_x t_x + \omega_y t_y\right) dS + \int_V \left(\omega_x b_x + \omega_y b_y\right) dV \\ &-\int_V \left[\frac{\partial \omega_x}{\partial x}\sigma_x + \frac{\partial \omega_y}{\partial y}\sigma_y + \left(\frac{\partial \omega_x}{\partial y} + \frac{\partial \omega_y}{\partial x}\right)\sigma_{xy}\right] dV = 0\end{aligned} \tag{2.4.15}$$

Finally, using (2.4.9) & (2.4.15)

$$\int_V \left(\tilde{\nabla}\boldsymbol{\omega}\right)^{\mathrm{T}} \boldsymbol{\sigma}\, dV = \int_S \boldsymbol{\omega}^{\mathrm{T}}\mathbf{t}\, dS + \int_V \boldsymbol{\omega}^{\mathrm{T}}\mathbf{b}\, dV \tag{2.4.16}$$

This is the weak form of the differential equations of mechanical equilibrium subjected to the boundary conditions given by Eqs. (2.4.7).

Considering the two-dimensional case where the displacements, strains, stresses, tractions and body forces do not depend on the z-coordinate.

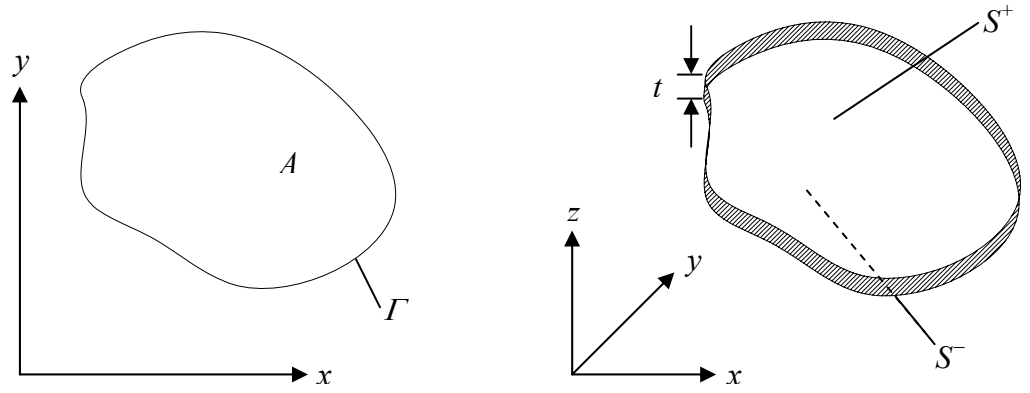

Figure 3.2:(a) Region A and boundary Γ for two-dimensional problems;
(b) Illustrations of upper surface S^+, lower surface S^- and thickness t.

As all integrands in Eq. (2.4.16) are independent on the z-coordinate, we obtain

$$\begin{aligned}&\int_V \left(\tilde{\nabla}\boldsymbol{\omega}\right)^{\mathrm{T}} \boldsymbol{\sigma}\, dV = \int_A \left[\int_Z \left(\tilde{\nabla}\boldsymbol{\omega}\right)^{\mathrm{T}} \boldsymbol{\sigma}\, dz\right] dA = \int_A \left(\tilde{\nabla}\boldsymbol{\omega}\right)^{\mathrm{T}} \boldsymbol{\sigma}\, t\, dZ \\ &\int_V \boldsymbol{\omega}^{\mathrm{T}}\mathbf{b}\, dV = \int_A \left[\int_Z \boldsymbol{\omega}^{\mathrm{T}}\mathbf{b}\, dz\right] dA = \int_A \boldsymbol{\omega}^{\mathrm{T}}\mathbf{b}\, t\, dV\end{aligned} \tag{2.4.17}$$

Considering the surface integral in Eq. (2.4.16), we get

$$\int_S \boldsymbol{\omega}^{\mathrm{T}}\mathbf{t}\, dS = \int_{S^+} \boldsymbol{\omega}^{\mathrm{T}}\mathbf{t}\, dS + \int_{S^-} \boldsymbol{\omega}^{\mathrm{T}}\mathbf{t}\, dS + \oint_\Gamma \left[\int_Z \boldsymbol{\omega}^{\mathrm{T}}\mathbf{t}\, dz\right] d\Gamma \tag{2.4.18}$$

The traction vector has components t_x and t_y. Along S^+ and S^- we have n_x=n_y=0, therefore

$$\mathbf{t} = \begin{bmatrix} t_x \\ t_y \end{bmatrix} = \begin{bmatrix} \sigma_{xz} n_z \\ \sigma_{yz} n_z \end{bmatrix} \tag{2.4.19}$$

For plane strain conditions, the components $\sigma_{xz} = \sigma_{xz}(x,y)$ and $\sigma_{yz} = \sigma_{yz}(x,y)$ may in general be different from zero. Along the upper surface S^+ we have $n_z = 1$, whereas for the lower surface S^- we have $n_z = -1$.

This leads to the conclusion that $\mathbf{t}^+ = -\mathbf{t}^-$ and as $\boldsymbol{\omega}$ is independent of the z-coordinate, Eq. (2.4.18) reduces to

$$\int_S \boldsymbol{\omega}^{\mathrm{T}} \mathbf{t} \; dS = \oint_\Gamma \boldsymbol{\omega}^{\mathrm{T}} \mathbf{t} \; t \; d\Gamma \tag{2.4.20}$$

Now, using Eqs. (2.4.20), (2.4.17) and assuming that the thickness t of the body is constant, the weak form for two-dimensional problems can be simplified into

$$\int_A \left(\widetilde{\nabla}\boldsymbol{\omega}\right)^{\mathrm{T}} \boldsymbol{\sigma} \; dA = \oint_\Gamma \boldsymbol{\omega}^{\mathrm{T}} \mathbf{t} \; d\Gamma + \int_A \boldsymbol{\omega}^{\mathrm{T}} \mathbf{b} \; dA \tag{2.4.21}$$

According to the Galerkin method, the arbitrary weight vector $\boldsymbol{\omega}$ is defined as

$$\boldsymbol{\omega} = \mathbf{N}_{\mathbf{m}} \bar{\boldsymbol{\omega}} \tag{2.4.22}$$

where,

$$\mathbf{N}_{\mathbf{m}} = \begin{bmatrix} N_1 & 0 & N_2 & 0 & N_3 & 0 & N_4 & 0 \\ 0 & N_1 & 0 & N_2 & 0 & N_3 & 0 & N_4 \end{bmatrix} \tag{2.4.23}$$

and

$$\bar{\boldsymbol{\omega}} = \begin{bmatrix} \omega_{\mathrm{x1}} & \omega_{\mathrm{y1}} & \omega_{\mathrm{x2}} & \omega_{\mathrm{y2}} & \omega_{\mathrm{x3}} & \omega_{\mathrm{y3}} & \omega_{\mathrm{x4}} & \omega_{\mathrm{y4}} \end{bmatrix}^{\mathrm{T}} \tag{2.4.24}$$

Hence $\boldsymbol{\omega}$ is arbitrary, $\bar{\boldsymbol{\omega}}$ is also arbitrary and it follows that

$$\widetilde{\nabla}\boldsymbol{\omega} = \mathbf{B}_{\mathbf{m}} \bar{\boldsymbol{\omega}} \tag{2.4.25}$$

where,

$$\mathbf{B_m} = \widetilde{\nabla}\mathbf{N_m}$$

$$= \begin{bmatrix} \frac{\partial}{\partial x}N_1 & 0 & \frac{\partial}{\partial x}N_2 & 0 & \frac{\partial}{\partial x}N_3 & 0 & \frac{\partial}{\partial x}N_4 & 0 \\ 0 & \frac{\partial}{\partial y}N_1 & 0 & \frac{\partial}{\partial y}N_2 & 0 & \frac{\partial}{\partial y}N_3 & 0 & \frac{\partial}{\partial y}N_4 \\ \frac{\partial}{\partial y}N_1 & \frac{\partial}{\partial x}N_1 & \frac{\partial}{\partial y}N_2 & \frac{\partial}{\partial x}N_2 & \frac{\partial}{\partial y}N_3 & \frac{\partial}{\partial x}N_3 & \frac{\partial}{\partial y}N_4 & \frac{\partial}{\partial x}N_4 \end{bmatrix} \quad (2.4.26)$$

Using (2.4.22) and (2.4.25), the weak form given by (2.4.21) becomes

$$\int_A \mathbf{B_m^T}\bar{\boldsymbol{\omega}}^{\mathbf{T}}\boldsymbol{\sigma}\, dA = \oint_\Gamma \mathbf{N_m^T}\bar{\boldsymbol{\omega}}^{\mathbf{T}}\mathbf{t}\, d\Gamma + \int_A \mathbf{N_m^T}\bar{\boldsymbol{\omega}}^{\mathbf{T}}\mathbf{b}\, dA \quad (2.4.27)$$

which can be further simplified to give

$$\int_A \mathbf{B_m^T}\boldsymbol{\sigma}\, dA = \oint_\Gamma \mathbf{N_m^T}\mathbf{t}\, d\Gamma + \int_A \mathbf{N_m^T}\mathbf{b}\, dA \quad (2.4.28)$$

If we are to express the total stress term in (2.4.28) in terms of strain, we have to first express it in terms of effective stress.

Bishop(1959) proposed a relationship between total stress and effective stress for unsaturated soil:

$$\boldsymbol{\sigma}^* = (\boldsymbol{\sigma} - \mathbf{m}p_a) + \chi(\mathbf{m}p_a - \mathbf{m}p_w) \quad (2.4.29)$$

$$\chi = \frac{\theta - \theta_r}{\theta_s - \theta_r} = \frac{S_r - S_{ri}}{1 - S_{ri}} \;;\; 0 \le \chi \le 1 \quad (2.4.30)$$

$$\mathbf{m} = \begin{bmatrix} 1 \\ 1 \\ 0 \end{bmatrix} \quad (2.4.31)$$

where:

θ : volumetric water content,
θ_s : saturated water content,
θ_r : residual water content,
S_r : degree of saturation, and is given by (2.3.32)
S_{ri} : residual degree of saturation,
$\boldsymbol{\sigma}$: total stress,
$\boldsymbol{\sigma}^*$: effective stress.

The nature of **m** implies that the fluids pressure only effects the normal stress components.

Eq. (2.4.29) can be manipulated and written in terms of total stress as:

$$\boldsymbol{\sigma} = \mathbf{m}p_a - \chi\left(\mathbf{m}p_a - \mathbf{m}p_w\right) + \boldsymbol{\sigma}^* \tag{2.4.32}$$

Inserting (2.4.32) into (2.4.28) results in

$$\int_A \mathbf{B}_\mathbf{m}^\mathrm{T}\left(\mathbf{m}p_a - \chi\left(\mathbf{m}p_a - \mathbf{m}p_w\right) + \boldsymbol{\sigma}^*\right)\, dA = \oint_\Gamma \mathbf{N}_\mathbf{m}^\mathrm{T}\mathbf{t}\, d\Gamma + \int_A \mathbf{N}_\mathbf{m}^\mathrm{T}\mathbf{b}\, dA \tag{2.4.33}$$

Simplifying (2.4.33) gives

$$\begin{aligned}&\int_A \mathbf{B}_\mathbf{m}^\mathrm{T}\mathbf{m}p_a\, dA - \int_A \mathbf{B}_\mathbf{m}^\mathrm{T}\chi\mathbf{m}p_a\, dA + \int_A \mathbf{B}_\mathbf{m}^\mathrm{T}\chi\mathbf{m}p_w\, dA + \int_A \mathbf{B}_\mathbf{m}^\mathrm{T}\boldsymbol{\sigma}^*\, dA \\ &= \oint_\Gamma \mathbf{N}_\mathbf{m}^\mathrm{T}\mathbf{t}\, d\Gamma + \int_A \mathbf{N}_\mathbf{m}^\mathrm{T}\mathbf{b}\, dA\end{aligned} \tag{2.4.34}$$

Effective stress term can be written in terms of Young's modulus and displacement as:

$$\boldsymbol{\sigma}^* = \mathbf{D}\boldsymbol{\varepsilon} - \mathbf{D}\boldsymbol{\varepsilon}_0 \tag{2.4.35}$$

Hence pane strain case is considered,

$$\boldsymbol{\varepsilon} = \begin{bmatrix} \varepsilon_x \\ \varepsilon_y \\ \gamma_{xy} \end{bmatrix} \tag{2.4.36}$$

$$\mathbf{D} = \frac{E}{(1+\upsilon)(1-2\upsilon)}\begin{bmatrix} 1-\upsilon & \upsilon & 0 \\ \upsilon & 1-\upsilon & 0 \\ 0 & 0 & \frac{1}{2}(1-2\upsilon) \end{bmatrix} \tag{2.4.37}$$

and $\boldsymbol{\varepsilon}_0$, the so-called initial strains, are the strains for zero stresses.

The displacement vector is given by

$$\mathbf{u} = \begin{bmatrix} u_x \\ u_y \end{bmatrix} \tag{2.4.38}$$

which is approximated by

$$\mathbf{u} = \mathbf{N}_\mathbf{m}\bar{\mathbf{u}} \tag{2.4.39}$$

where $\mathbf{N_m}$ is given by Eq. (2.4.23) as

$$\mathbf{N_m} = \begin{bmatrix} N_1 & 0 & N_2 & 0 & N_3 & 0 & N_4 & 0 \\ 0 & N_1 & 0 & N_2 & 0 & N_3 & 0 & N_4 \end{bmatrix}$$

and

$$\bar{\mathbf{u}} = \begin{bmatrix} u_{x1} & u_{y1} & u_{x2} & u_{y2} & u_{x3} & u_{y3} & u_{x4} & u_{y4} \end{bmatrix}^T \tag{2.4.40}$$

Strains $\boldsymbol{\varepsilon}$ can be written in terms of displacements as

$$\boldsymbol{\varepsilon} = \tilde{\nabla}\mathbf{u} \tag{2.4.41}$$

From (2.4.39) and (2.4.26) we obtain

$$\boldsymbol{\varepsilon} = \mathbf{B_m}\bar{\mathbf{u}} \tag{2.4.42}$$

So, (2.4.35) takes the form

$$\boldsymbol{\sigma}^* = \mathbf{D}\mathbf{B_m}\bar{\mathbf{u}} - \mathbf{D}\boldsymbol{\varepsilon}_0 \tag{2.4.43}$$

Inserting (2.4.43) into (2.4.34) results in

$$\begin{aligned} &\int_A \mathbf{B_m^T}\mathbf{m}p_a \, dA - \int_A \mathbf{B_m^T}\chi\mathbf{m}p_a \, dA + \int_A \mathbf{B_m^T}\chi\mathbf{m}p_w \, dA + \int_A \mathbf{B_m^T}\mathbf{D}\mathbf{B_m}\bar{\mathbf{u}} \, dA - \int_A \mathbf{B_m^T}\mathbf{D}\boldsymbol{\varepsilon}_0 \, dA \\ &= \oint_\Gamma \mathbf{N_m^T}\mathbf{t} \, d\Gamma + \int_A \mathbf{N_m^T}\mathbf{b} \, dA \end{aligned} \tag{2.4.44}$$

Rearranging (2.4.44) gives

$$\begin{aligned} &\int_A \mathbf{B_m^T}\mathbf{m}p_a \, dA - \int_A \mathbf{B_m^T}\chi\mathbf{m}p_a \, dA + \int_A \mathbf{B_m^T}\chi\mathbf{m}p_w \, dA + \left(\int_A \mathbf{B_m^T}\mathbf{D}\mathbf{B_m} \, dA \right)\bar{\mathbf{u}} \\ &= \oint_\Gamma \mathbf{N_m^T}\mathbf{t} \, d\Gamma + \int_A \mathbf{N_m^T}\mathbf{b} \, dA + \int_A \mathbf{B_m^T}\mathbf{D}\boldsymbol{\varepsilon}_0 \, dA \end{aligned} \tag{2.4.45}$$

Discretizing for pressure of air and pressure of water, (2.4.45) becomes

$$\begin{aligned} &\int_A \mathbf{B_m^T}\mathbf{m}\left(\mathbf{N_n}\overline{\mathbf{p_a}}\right) dA - \int_A \mathbf{B_m^T}\chi\mathbf{m}\left(\mathbf{N_n}\overline{\mathbf{p_a}}\right) dA + \int_A \mathbf{B_m^T}\chi\mathbf{m}\left(\mathbf{N_n}\overline{\mathbf{p_w}}\right) dA \\ &+ \left(\int_A \mathbf{B_m^T}\mathbf{D}\mathbf{B_m} \, dA \right)\bar{\mathbf{u}} = \oint_\Gamma \mathbf{N_m^T}\mathbf{t} \, d\Gamma + \int_A \mathbf{N_m^T}\mathbf{b} \, dA + \int_A \mathbf{B_m^T}\mathbf{D}\boldsymbol{\varepsilon}_0 \, dA \end{aligned} \tag{2.4.46}$$

where $\mathbf{N_n}$ is given by (2.3.4) as

$$\mathbf{N}_{\mathrm{n}} = \begin{bmatrix} N_1 & N_2 & N_3 & N_4 \end{bmatrix}$$

and $\overline{\mathbf{p}_a}$ and $\overline{\mathbf{p}_w}$ are given by (2.3.25)-(2.3.26) as

$$\overline{\mathbf{p}_{\mathrm{a}}} = \begin{bmatrix} p_{a_1} \\ p_{a_2} \\ p_{a_3} \\ p_{a_4} \end{bmatrix} \; ; \; \overline{\mathbf{p}_{\mathrm{w}}} = \begin{bmatrix} p_{w_1} \\ p_{w_2} \\ p_{w_3} \\ p_{w_4} \end{bmatrix}$$

Equation (2.4.46) can be simplified and written as

$$\begin{aligned} &\int_A \mathbf{B}_{\mathbf{m}}^{\mathrm{T}} \mathbf{m} \mathbf{N}_{\mathbf{n}} \, dA \, \overline{\mathbf{p}_{\mathbf{a}}} - \int_A \mathbf{B}_{\mathbf{m}}^{\mathrm{T}} \chi \mathbf{m} \mathbf{N}_{\mathbf{n}} \, dA \, \overline{\mathbf{p}_{\mathbf{a}}} + \int_A \mathbf{B}_{\mathbf{m}}^{\mathrm{T}} \chi \mathbf{m} \mathbf{N}_{\mathbf{n}} \, dA \, \overline{\mathbf{p}_{\mathbf{w}}} \\ &+ \int_A \mathbf{B}_{\mathbf{m}}^{\mathrm{T}} \mathbf{D} \mathbf{B}_{\mathbf{m}} \, dA \, \bar{\mathbf{u}} = \oint_\Gamma \mathbf{N}_{\mathbf{m}}^{\mathrm{T}} \mathbf{t} \, d\Gamma + \int_A \mathbf{N}_{\mathbf{m}}^{\mathrm{T}} \mathbf{b} \, dA + \int_A \mathbf{B}_{\mathbf{m}}^{\mathrm{T}} \mathbf{D} \boldsymbol{\varepsilon}_{\mathbf{0}} \, dA \end{aligned} \tag{2.4.47}$$

Taking partial derivative of (2.4.47) with respect to time and simplifying,

$$\begin{aligned} &\int_A \mathbf{B}_{\mathbf{m}}^{\mathrm{T}} \mathbf{m} \mathbf{N}_{\mathbf{n}} \, dA \, \frac{\partial}{\partial t} \overline{\mathbf{p}_{\mathbf{a}}} - \int_A \mathbf{B}_{\mathbf{m}}^{\mathrm{T}} \chi \mathbf{m} \mathbf{N}_{\mathbf{n}} \, dA \, \frac{\partial}{\partial t} \overline{\mathbf{p}_{\mathbf{a}}} + \int_A \mathbf{B}_{\mathbf{m}}^{\mathrm{T}} \chi \mathbf{m} \mathbf{N}_{\mathbf{n}} \, dA \, \frac{\partial}{\partial t} \overline{\mathbf{p}_{\mathbf{w}}} \\ &+ \int_A \mathbf{B}_{\mathbf{m}}^{\mathrm{T}} \mathbf{D} \mathbf{B}_{\mathbf{m}} \, dA \, \frac{\partial}{\partial t} \bar{\mathbf{u}} = \oint_\Gamma \mathbf{N}_{\mathbf{m}}^{\mathrm{T}} \frac{\partial}{\partial t} \mathbf{t} \, d\Gamma + \int_A \mathbf{N}_{\mathbf{m}}^{\mathrm{T}} \frac{\partial}{\partial t} \mathbf{b} \, dA + \int_A \mathbf{B}_{\mathbf{m}}^{\mathrm{T}} \mathbf{D} \frac{\partial}{\partial t} \boldsymbol{\varepsilon}_{\mathbf{0}} \, dA \end{aligned} \tag{2.4.48}$$

Equation (2.4.48) can be more concisely written as

$$\left(\mathbf{C}_{\mathbf{2}}^{\mathbf{1}} - \mathbf{C}_{\mathbf{2}}^{\mathbf{2}} \right) \frac{\partial}{\partial t} \overline{\mathbf{p}_{\mathbf{a}}} + \mathbf{C}_{\mathbf{2}}^{\mathbf{2}} \frac{\partial}{\partial t} \overline{\mathbf{p}_{\mathbf{w}}} + \mathbf{C}_{\mathbf{2}}^{\mathbf{3}} \frac{\partial}{\partial t} \bar{\mathbf{u}} = \mathbf{C}_{\mathbf{2}}^{\mathbf{4}} + \mathbf{C}_{\mathbf{2}}^{\mathbf{5}} + \mathbf{C}_{\mathbf{2}}^{\mathbf{6}} \tag{2.4.49}$$

where

$$\begin{aligned} \mathbf{C}_{\mathbf{2}}^{\mathbf{1}} &= \int_A \mathbf{B}_{\mathbf{m}}^{\mathrm{T}} \mathbf{m} \mathbf{N}_{\mathbf{n}} \, dA & \mathbf{C}_{\mathbf{2}}^{\mathbf{4}} &= \oint_\Gamma \mathbf{N}_{\mathbf{m}}^{\mathrm{T}} \frac{\partial}{\partial t} \mathbf{t} \, d\Gamma \\ \mathbf{C}_{\mathbf{2}}^{\mathbf{2}} &= \int_A \mathbf{B}_{\mathbf{m}}^{\mathrm{T}} \chi \mathbf{m} \mathbf{N}_{\mathbf{n}} \, dA & \mathbf{C}_{\mathbf{2}}^{\mathbf{5}} &= \int_A \mathbf{N}_{\mathbf{m}}^{\mathrm{T}} \frac{\partial}{\partial t} \mathbf{b} \, dA \\ \mathbf{C}_{\mathbf{2}}^{\mathbf{3}} &= \int_A \mathbf{B}_{\mathbf{m}}^{\mathrm{T}} \mathbf{D} \mathbf{B}_{\mathbf{m}} \, dA & \mathbf{C}_{\mathbf{2}}^{\mathbf{6}} &= \int_A \mathbf{B}_{\mathbf{m}}^{\mathrm{T}} \mathbf{D} \frac{\partial}{\partial t} \boldsymbol{\varepsilon}_{\mathbf{0}} \, dA \end{aligned} \tag{2.4.50}$$

and χ, S_r are given by (2.4.30) and (2.3.31) respectively.

3.5 Formulation of air mass balance equation

The continuity of air mass filling the soil voids is given by:

$$\frac{\partial}{\partial t}\left[\rho_a n\left(1-S_r+HS_r\right)\right]+\operatorname{div}\left[\rho_a\left(\mathbf{v}_{\mathrm{a}}+H\mathbf{v}_{\mathbf{w}}\right)\right]=0 \qquad (2.5.1)$$

where n is the porosity and ρ_a is the density of air.

$\mathbf{v_w}$ is given by (2.3.7) as

$$\mathbf{v}_{\mathrm{w}}=\begin{bmatrix} v_{wx} \\ v_{wy} \end{bmatrix}$$

similarly

$$\mathbf{v}_{\mathrm{a}}=\begin{bmatrix} v_{ax} \\ v_{ay} \end{bmatrix} \qquad (2.5.2)$$

It is assumed that air behaves as an ideal gas and hence density and pressure are related as follows:

$$\rho_a=\frac{M}{RT}p_a \qquad (2.5.3)$$

where $T(^{\mathrm{o}}\mathrm{K})$ is the absolute temperature, R the gas constant and M is the molecular weight of air ($M/(RT)$ is the compressibility of air, assumed constant).

Substituting Eq. (2.5.3) into Eq. (2.5.1):

$$\frac{\partial}{\partial t}\left[p_a n\left(1-S_r+HS_r\right)\right]+\operatorname{div}\left[p_a\left(\mathbf{v}_{\mathrm{a}}+H\mathbf{v}_{\mathrm{w}}\right)\right]=0 \qquad (2.5.4)$$

Simplifying (2.5.4) further:

$$\frac{\partial}{\partial t}\left[p_a n-p_a nS_r+Hp_a nS_r\right]+\operatorname{div}\left[p_a\mathbf{v}_{\mathbf{a}}\right]+\operatorname{div}\left[Hp_a\mathbf{v}_{\mathbf{w}}\right]=0 \qquad (2.5.5)$$

Multiplying (2.5.5) by an arbitrary function ϕ – the weight function – and integrating over the region (limiting the scope for two-dimensional problems and considering constant element thickness) gives

$$\int_A \phi\frac{\partial}{\partial t}\left[p_a n-p_a nS_r+Hp_a nS_r\right]\,dA+\int_A \phi\,\operatorname{div}\left[p_a\mathbf{v}_{\mathbf{a}}\right]\,dA+\int_A \phi\,\operatorname{div}\left[Hp_a\mathbf{v}_{\mathbf{w}}\right]\,dA=0 \qquad (2.5.6)$$

Integrating by parts the second and third terms of (2.5.6) by Green-Gauss theorem gives

$$\begin{aligned}\int_A \phi \ \mathrm{div}\left[p_a \mathbf{v_a}\right]\ dA &= \oint_\Gamma \phi p_a \mathbf{v_a^T n}\ d\Gamma - \int_A \left(\nabla\phi\right)^{\mathrm{T}} p_a \mathbf{v_a}\ dA \\ \int_A \phi \ \mathrm{div}\left[Hp_a \mathbf{v_w}\right]\ dA &= \oint_\Gamma \phi Hp_a \mathbf{v_w^T n}\ d\Gamma - \int_A \left(\nabla\phi\right)^{\mathrm{T}} Hp_a \mathbf{v_w}\ dA\end{aligned} \tag{2.5.7}$$

Using (2.5.7), (2.5.6) can be written as

$$\begin{aligned}&\int_A \phi \frac{\partial}{\partial t}\left[p_a n - p_a n S_r + Hp_a n S_r\right]\ dA + \oint_\Gamma \phi p_a \mathbf{v_a^T n}\ d\Gamma - \int_A \left(\nabla\phi\right)^{\mathrm{T}} p_a \mathbf{v_a}\ dA \\ &+\oint_\Gamma \phi Hp_a \mathbf{v_w^T n}\ d\Gamma - \int_A \left(\nabla\phi\right)^{\mathrm{T}} Hp_a \mathbf{v_w}\ dA = 0\end{aligned} \tag{2.5.8}$$

Using (2.3.12) - (2.3.14)

$$\begin{aligned}\bar{\boldsymbol{\varphi}}^{\mathbf{T}}\Bigg[&\int_A \mathbf{N_n^T} \frac{\partial}{\partial t}\left[p_a n - p_a n S_r + Hp_a n S_r\right]\ dA + \oint_\Gamma \mathbf{N_n^T} p_a \mathbf{v_a^T n}\ d\Gamma - \int_A \mathbf{B_n^T} p_a \mathbf{v_a}\ dA \\ &+\oint_\Gamma \mathbf{N_n^T} Hp_a \mathbf{v_w^T n}\ d\Gamma - \int_A \mathbf{B_n^T} Hp_a \mathbf{v_w}\ dA\Bigg] = 0\end{aligned} \tag{2.5.9}$$

As the Eq. (2.5.9) should hold for arbitrary $\bar{\boldsymbol{\varphi}}^{\mathbf{T}}$ matrices, it can be concluded that:

$$\begin{aligned}&\int_A \mathbf{N_n^T} \frac{\partial}{\partial t}\left[p_a n - p_a n S_r + Hp_a n S_r\right]\ dA + \oint_\Gamma \mathbf{N_n^T} p_a \mathbf{v_a^T n}\ d\Gamma + \oint_\Gamma \mathbf{N_n^T} Hp_a \mathbf{v_w^T n}\ d\Gamma \\ &-\int_A \mathbf{B_n^T} p_a \mathbf{v_a}\ dA - \int_A \mathbf{B_n^T} Hp_a \mathbf{v_w}\ dA = 0\end{aligned} \tag{2.5.10}$$

From (2.3.20)-(2.3.21)

$$\mathbf{v}_{\mathrm{w}} = -K_w\left(\frac{1}{\gamma_w}\nabla p_w + \nabla z\right); \qquad \nabla p_w = \begin{bmatrix}\frac{\partial}{\partial x} \\ \frac{\partial}{\partial y}\end{bmatrix} p_w = \begin{bmatrix}\frac{\partial p_w}{\partial x} \\ \frac{\partial p_w}{\partial y}\end{bmatrix}$$

Similarly, motion of air can be described by a generalization of Darcy's law

$$\mathbf{v}_{\mathrm{a}} = -K_a\left(\frac{1}{\gamma_a}\nabla p_a + \nabla z\right) \tag{2.5.11}$$

where K_a is the coefficient of permeability and γ_a the specific weight of air.

Brun (1989) proposed a relationship for coefficient of permeability interms of suction as

$$K_a = \frac{A_a K_{as}}{A_a + \left(C_a \left(p_a - p_w\right)\right)^{-B_a}} \tag{2.5.12}$$

where A_a, B_a, C_a and K_{as} are constants.

Also, from (2.3.18)

$$q_w = \mathbf{v}_\mathbf{w}^\mathrm{T}\mathbf{n}$$

similarly

$$q_a = \mathbf{v}_\mathbf{a}^\mathrm{T}\mathbf{n} \tag{2.5.13}$$

where q_a is the air flux across the boundary.

Now, (2.5.10) can be further simplified and written as

$$\begin{aligned}
&\int_A \mathbf{N}_\mathbf{n}^\mathrm{T} p_a \frac{\partial}{\partial t} n \; dA + \int_A \mathbf{N}_\mathbf{n}^\mathrm{T} n \frac{\partial}{\partial t} p_a \; dA \\
&+ \left(H - 1\right) \int_A \mathbf{N}_\mathbf{n}^\mathrm{T} p_a n \frac{\partial}{\partial t} S_r \; dA \\
&+ \left(H - 1\right) \int_A \mathbf{N}_\mathbf{n}^\mathrm{T} p_a S_r \frac{\partial}{\partial t} n \; dA \\
&+ \left(H - 1\right) \int_A \mathbf{N}_\mathbf{n}^\mathrm{T} n S_r \frac{\partial}{\partial t} p_a \; dA \\
&+ \oint_\Gamma \mathbf{N}_\mathbf{n}^\mathrm{T} p_a q_a \; d\boldsymbol{\Gamma} + \oint_\Gamma \mathbf{N}_\mathbf{n}^\mathrm{T} H p_a q_w \; d\boldsymbol{\Gamma} \\
&+ \int_A \frac{1}{\gamma_a} \mathbf{B}_\mathbf{n}^\mathrm{T} p_a K_a \nabla p_a \; dA + \int_A \mathbf{B}_\mathbf{n}^\mathrm{T} p_a K_a \nabla z \; dA \\
&+ \int_A \frac{1}{\gamma_w} \mathbf{B}_\mathbf{n}^\mathrm{T} H p_a K_w \nabla p_w \; dA + \int_A \mathbf{B}_\mathbf{n}^\mathrm{T} H p_a K_w \nabla z \; dA = 0
\end{aligned} \tag{2.5.14}$$

Expressing porosity in terms of displacement and using (2.3.32)

$$
\begin{aligned}
&\int_A \mathbf{N_n^T} p_a \frac{\partial}{\partial t}\left(\mathbf{m^T}\widetilde{\nabla}\mathbf{u}\right)\, dA + \int_A \mathbf{N_n^T} n \frac{\partial}{\partial t} p_a\, dA \\
&+\left(H-1\right)\int_A \mathbf{N_n^T} p_a n \frac{\partial S_r}{\partial p_w}\frac{\partial}{\partial t} p_w\, dA \\
&+\left(H-1\right)\int_A \mathbf{N_n^T} p_a S_r \frac{\partial}{\partial t}\left(\mathbf{m^T}\widetilde{\nabla}\mathbf{u}\right)\, dA \\
&+\left(H-1\right)\int_A \mathbf{N_n^T}\left(\mathbf{m^T}\widetilde{\nabla}\mathbf{u}\right) S_r \frac{\partial}{\partial t}\left(p_a\right)\, dA \\
&+\oint_{\Gamma} \mathbf{N_n^T} p_a q_a\, d\boldsymbol{\Gamma} + \oint_{\Gamma} \mathbf{N_n^T} H p_a q_w\, d\boldsymbol{\Gamma} \\
&+\int_A \frac{1}{\gamma_a}\mathbf{B_n^T} p_a K_a \nabla p_a\, dA + \int_A \mathbf{B_n^T} p_a K_a \nabla z\, dA \\
&+\int_A \frac{1}{\gamma_w}\mathbf{B_n^T} H p_a K_w \nabla p_w\, dA + \int_A \mathbf{B_n^T} H p_a K_w \nabla z\, dA = 0
\end{aligned}
\tag{2.5.15}
$$

Discretizing for pressure of air and pressure of water and using (2.4.42), equation (2.5.15) becomes

$$
\begin{aligned}
&\int_A \mathbf{N_n^T N_n}\overline{\mathbf{p_a}} \frac{\partial}{\partial t}\left(\mathbf{m^T B_m u}\right)\, dA + \int_A \mathbf{N_n^T} n \frac{\partial}{\partial t}\left(\mathbf{N_n}\overline{\mathbf{p_a}}\right)\, dA \\
&+\left(H-1\right)\int_A \mathbf{N_n^T N_n}\overline{\mathbf{p_a}} n \frac{\partial S_r}{\partial p_w}\frac{\partial}{\partial t}\left(\mathbf{N_n}\overline{\mathbf{p_w}}\right)\, dA \\
&+\left(H-1\right)\int_A \mathbf{N_n^T N_n}\overline{\mathbf{p_a}} S_r \frac{\partial}{\partial t}\left(\mathbf{m^T B_m u}\right)\, dA \\
&+\left(H-1\right)\int_A \mathbf{N_n^T}\left(\mathbf{m^T B_m u}\right) S_r \frac{\partial}{\partial t}\left(\mathbf{N_n}\overline{\mathbf{p_a}}\right)\, dA \\
&+\oint_{\Gamma} \mathbf{N_n^T N_n}\overline{\mathbf{p_a}} q_a\, d\boldsymbol{\Gamma} + \oint_{\Gamma} H\mathbf{N_n^T N_n}\overline{\mathbf{p_a}} q_w\, d\boldsymbol{\Gamma} \\
&+\int_A \frac{1}{\gamma_a}\mathbf{B_n^T N_n}\overline{\mathbf{p_a}} K_a \nabla\left(\mathbf{N_n}\overline{\mathbf{p_a}}\right)\, dA + \int_A \mathbf{B_n^T N_n}\overline{\mathbf{p_a}} K_a \nabla z\, dA \\
&+\int_A H\frac{1}{\gamma_w}\mathbf{B_n^T N_n}\overline{\mathbf{p_a}} K_w \nabla\left(\mathbf{N_n}\overline{\mathbf{p_w}}\right)\, dA + \int_A H\mathbf{B_n^T N_n}\overline{\mathbf{p_a}} K_w \nabla z\, dA = 0
\end{aligned}
\tag{2.5.16}
$$

Simplifying (2.5.16)

$$\begin{aligned}
&\int_A \mathbf{N_n^T N_n} \overline{\mathbf{p_a}} \mathbf{m^T B_m} \frac{\partial}{\partial t}(\mathbf{u})\, dA + \int_A \mathbf{N_n^T} n \mathbf{N_n} \frac{\partial}{\partial t}\left(\overline{\mathbf{p_a}}\right) dA \\
&+ (H-1) \int_A \mathbf{N_n^T N_n} \overline{\mathbf{p_a}} n \frac{\partial S_r}{\partial p_w} \mathbf{N_n} \frac{\partial}{\partial t}\left(\overline{\mathbf{p_w}}\right) dA \\
&+ (H-1) \int_A \mathbf{N_n^T} p_a S_r \mathbf{m^T B_m} \frac{\partial}{\partial t}(\mathbf{u})\, dA \\
&+ (H-1) \int_A \mathbf{N_n^T} \left(\mathbf{m^T B_m u}\right) S_r \mathbf{N_n} \frac{\partial}{\partial t}\left(\overline{\mathbf{p_a}}\right) dA \qquad (2.5.17) \\
&+ \oint_\Gamma \mathbf{N_n^T N_n} \overline{\mathbf{p_a}} q_a \, d\boldsymbol{\Gamma} + \oint_\Gamma \mathbf{N_n^T} H \mathbf{N_n} \overline{\mathbf{p_a}} q_w \, d\boldsymbol{\Gamma} \\
&+ \int_A \frac{1}{\gamma_a} \mathbf{B_n^T N_n} \overline{\mathbf{p_a}} K_a \mathbf{B_n} \overline{\mathbf{p_a}}\, dA + \int_A \mathbf{B_n^T N_n} \overline{\mathbf{p_a}} K_a \nabla z\, dA \\
&+ \int_A \frac{1}{\gamma_w} \mathbf{B_n^T} H p_a K_w \mathbf{B_n} \overline{\mathbf{p_w}}\, dA + \int_A \mathbf{B_n^T} H \mathbf{N_n} \overline{\mathbf{p_a}} K_w \nabla z\, dA = 0
\end{aligned}$$

Equation (2.5.17) can be more concisely written as

$$\mathbf{C_3^1}\ \frac{\partial}{\partial t}\left(\overline{\mathbf{u}}\right) + \mathbf{C_3^2}\ \frac{\partial}{\partial t}\left(\overline{\mathbf{p_a}}\right) + \mathbf{C_3^3}\ \frac{\partial}{\partial t}\left(\overline{\mathbf{p_w}}\right) + \mathbf{C_3^4}\overline{\mathbf{p_a}} + \mathbf{C_3^5}\overline{\mathbf{p_w}} + \mathbf{C_3^6}\ + \mathbf{C_3^7}\ = 0 \quad (2.5.18)$$

where,

$$\begin{aligned}
\mathbf{C_3^1} &= \int_A \mathbf{N_n^T N_n} \overline{\mathbf{p_a}} \mathbf{m^T B_m}\, dA \ + \ (H-1) \int_A \mathbf{N_n^T} p_a S_r \mathbf{m^T B_m}\, dA \\
\mathbf{C_3^2} &= \int_A \mathbf{N_n^T} n \mathbf{N_n}\, dA \ + \ (H-1) \int_A \mathbf{N_n^T} \left(\mathbf{m^T B_m u}\right) S_r \mathbf{N_n}\, dA \\
\mathbf{C_3^3} &= (H-1) \int_A \mathbf{N_n^T N_n} \overline{\mathbf{p_a}} n \frac{\partial S_r}{\partial p_w} \mathbf{N_n}\, dA \\
\mathbf{C_3^4} &= \int_A \frac{1}{\gamma_a} \mathbf{B_n^T N_n} \overline{\mathbf{p_a}} K_a \mathbf{B_n}\, dA \qquad (2.5.19) \\
\mathbf{C_3^5} &= \int_A \frac{1}{\gamma_w} \mathbf{B_n^T} H p_a K_w \mathbf{B_n}\, dA \\
\mathbf{C_3^6} &= \oint_\Gamma \mathbf{N_n^T N_n} \overline{\mathbf{p_a}} q_a \, d\boldsymbol{\Gamma} + \oint_\Gamma \mathbf{N_n^T} H \mathbf{N_n} \overline{\mathbf{p_a}} q_w \, d\boldsymbol{\Gamma} \\
\mathbf{C_3^7} &= \int_A \mathbf{B_n^T N_n} \overline{\mathbf{p_a}} K_a \nabla z\, dA + \int_A \mathbf{B_n^T} H \mathbf{N_n} \overline{\mathbf{p_a}} K_w \nabla z\, dA
\end{aligned}$$

3.6 A coupled solution method for the proposed equations

Recalling the Equations (2.3.39), (2.4.49) and (2.5.18):

$$\mathbf{C}_1^1 \frac{\partial}{\partial t}\left(\overline{\mathbf{p}_\mathrm{w}}\right) + \mathbf{C}_1^2 \frac{\partial}{\partial t}\left(\overline{\mathbf{u}}\right) + \mathbf{C}_1^3 + \mathbf{C}_1^4 \overline{\mathbf{p}_\mathrm{w}} + \mathbf{C}_1^5 = 0$$

$$\left(\mathbf{C}_2^1 - \mathbf{C}_2^2\right)\frac{\partial}{\partial t}\overline{\mathbf{p}_\mathrm{a}} + \mathbf{C}_2^2 \frac{\partial}{\partial t}\overline{\mathbf{p}_\mathrm{w}} + \mathbf{C}_2^3 \frac{\partial}{\partial t}\overline{\mathbf{u}} \;=\; \mathbf{C}_2^4 + \mathbf{C}_2^5 + \mathbf{C}_2^6$$

$$\mathbf{C}_3^1 \;\frac{\partial}{\partial t}\left(\overline{\mathbf{u}}\right) + \mathbf{C}_3^2 \;\frac{\partial}{\partial t}\left(\overline{\mathbf{p}_\mathrm{a}}\right) + \mathbf{C}_3^3 \;\frac{\partial}{\partial t}\left(\overline{\mathbf{p}_\mathrm{w}}\right) + \mathbf{C}_3^4 \overline{\mathbf{p}_\mathrm{a}} + \mathbf{C}_3^5 \overline{\mathbf{p}_\mathrm{w}} + \mathbf{C}_3^6 \;+ \mathbf{C}_3^7 \;= 0$$

The Equations (2.3.39), (2.4.49) and (2.5.18) can be combined and written as one matrix equation:

$$\begin{bmatrix} \mathbf{C}_3^2 & \mathbf{C}_3^3 & \mathbf{C}_3^1 \\ 0 & \mathbf{C}_1^1 & \mathbf{C}_1^2 \\ \left(\mathbf{C}_2^1 - \mathbf{C}_2^2\right) & \mathbf{C}_2^2 & \mathbf{C}_2^3 \end{bmatrix} \times \frac{\partial}{\partial t}\begin{Bmatrix} \overline{\mathbf{p}_\mathrm{a}} \\ \overline{\mathbf{p}_\mathrm{w}} \\ \overline{\mathbf{u}} \end{Bmatrix} + \begin{bmatrix} \mathbf{C}_3^4 & \mathbf{C}_3^5 & 0 \\ 0 & \mathbf{C}_1^4 & 0 \\ 0 & 0 & 0 \end{bmatrix} \times \begin{Bmatrix} \overline{\mathbf{p}_\mathrm{a}} \\ \overline{\mathbf{p}_\mathrm{w}} \\ \overline{\mathbf{u}} \end{Bmatrix} = \begin{Bmatrix} -\mathbf{C}_3^6 - \mathbf{C}_3^7 \\ -\mathbf{C}_1^3 - \mathbf{C}_1^5 \\ \mathbf{C}_2^4 + \mathbf{C}_2^5 + \mathbf{C}_2^6 \end{Bmatrix} \quad (2.6.1)$$

Now equation (2.6.1) can be written in a more generalized form as:

$$[\mathbf{M}]\{\dot{\mathbf{d}}\} \;+\; [\mathbf{K}]\{\mathbf{d}\} \;=\; \{\mathbf{F}\} \qquad (2.6.2)$$

where **M** is the system capacity matrix, **K** is the system conductivity matrix, **F** is the system flux vector and **d** is the matrix of primary variables.

Numerical time integration is performed by using the backward Euler method to solve the above semi-discrete parabolic equation. Figure 3.3 shows the flow chart of the process to solve the proposed coupled system of equations.

To find initial rate of change of degree of freedoms

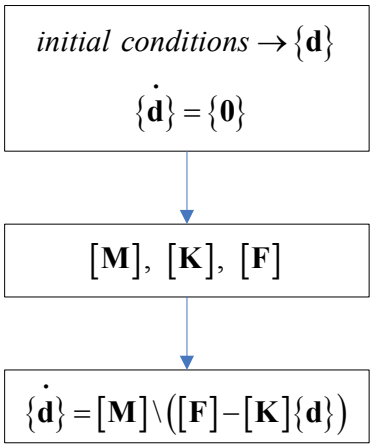

Iterations at time $t = n + 1$

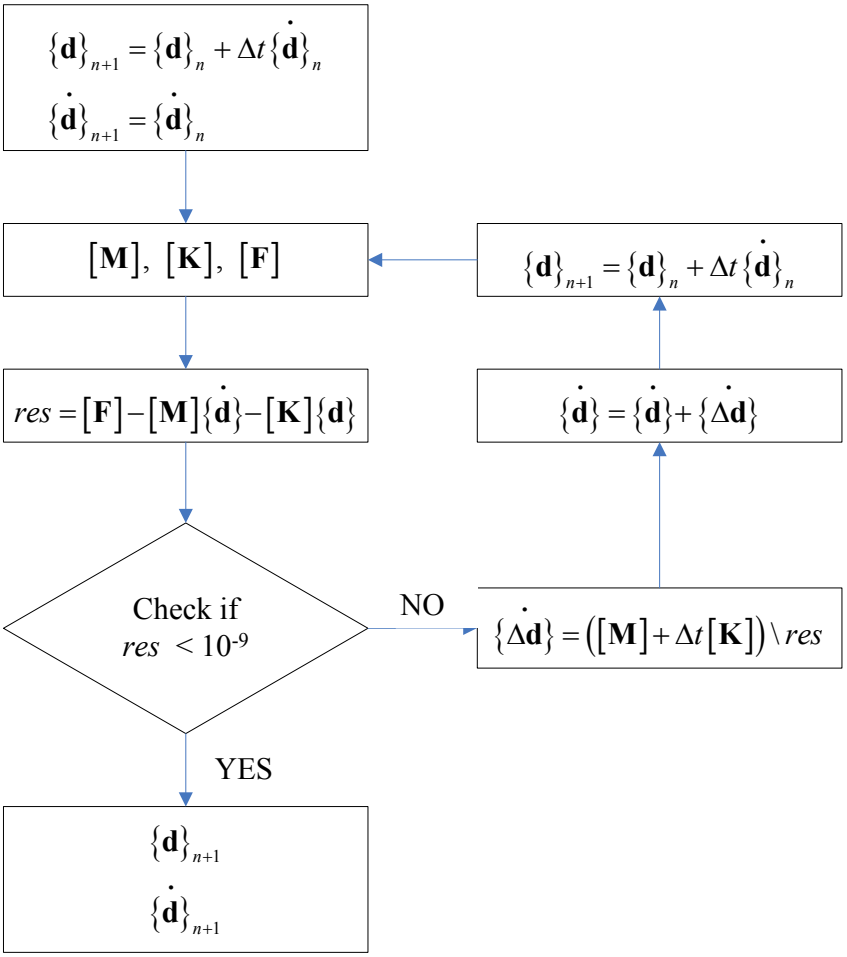

Figure 3.3: Flow chart of the process to solve the proposed coupled system of equations

3.7 Application of Model

A soil-slope problem in residual soil is taken for the demonstration. The rainfall perturbation is taken as the forcing function that affects the flow regime as well as soil deformation. The displacement boundary conditions and slope dimensions are displayed in the Figure 1. No flow boundary is assumed on either side of the slope (*af*, *de* and *fe*). Material properties input are shown in Table 2. Rainfall intensity of 20 mm/hr is applied to surfaces *ab*, *bc* and *cd* of the slope. For the slope in residual soil, pore-air pressure is assumed to be zero. Initial water pressure is illustrated in Figure 2 as a contour plot. The results from the code, with rainfall infiltration for 24 hours, are presented here. The material properties of the chosen residual soil are given in Table 3.1.

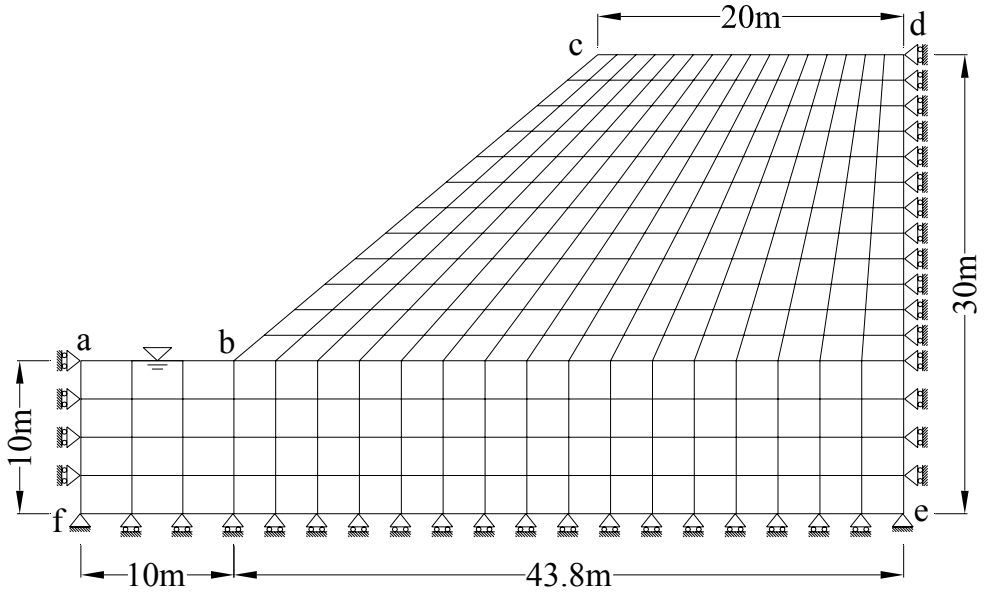

Figure 3.4: Domain of Analysis with displacement BCs.

Water permeability	$K_{ws} = 5\times10^{-5}$, $A_w = 1.0$, $B_w = 0.96$, $C_w = 5.16\text{e-}4$
Degree of saturation	$S_{ri} = 0.08$, $S_{rs} = 1.0$, $A_w = 0.96$, $B_w = 3.5$, $C_w = 5.00\text{e-}5$
Void ratio – state surface	a = -7.58e-8, b = -6.45e-8, c = 1.61e-10, d = 0.6462
Young's modulus	$E = 7.88\times10^{9}$ N/m^3
Poisson's ratio	$\mu = 0.35$
Rainfall intensity	20 mm/hr

Table 3.1: Material Properties

Chapter 4

Results and Discussion

With the Dirichlet boundary condition on the nodes of the boundary *ed* when the water flows into slope, and Neuman Boundary condition (impervious boundary) when the water begins to discharge from the slope, contours of initial pore pressure in the domain of analysis is shown in Figure 4.1.

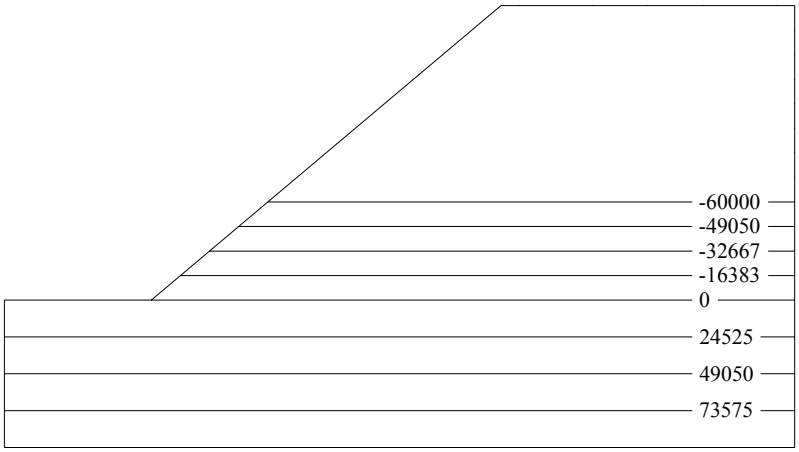

Figure 4.1: Contour lines of initial pore-pressure (in Pascal)

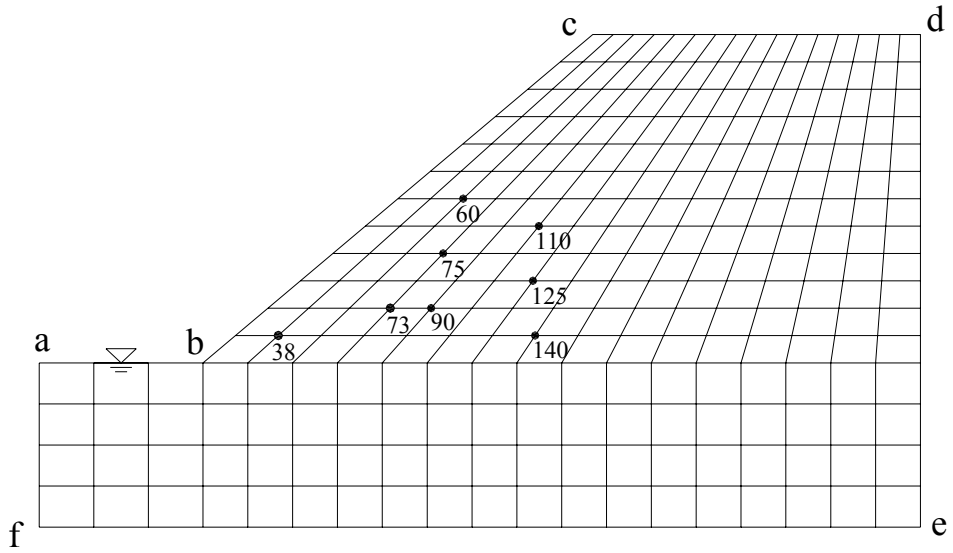

Figure 4.2: Domain of Analysis showing chosen nodes

Results from the infiltration induced changes in matric suction are presented in Figure 4.3(a) and 4.3(b). Two nodes (node 38 and 73) were carefully selected to describe the effects of infiltration. The matric suction decreases with time due to infiltration and eventually converges towards zero. The response is different according to the distance from the slope surface and initial conditions of water pressure at the nodes. For the node closer to the surface (node 38), the reduction in matric suction starts immediately whereas for the node 73, suction remains constant until 8 hours of consistent rainfall and drops rapidly as shown in Figure 4.3(b) as it takes more time for the seeping rainwater to reach a deeper location.

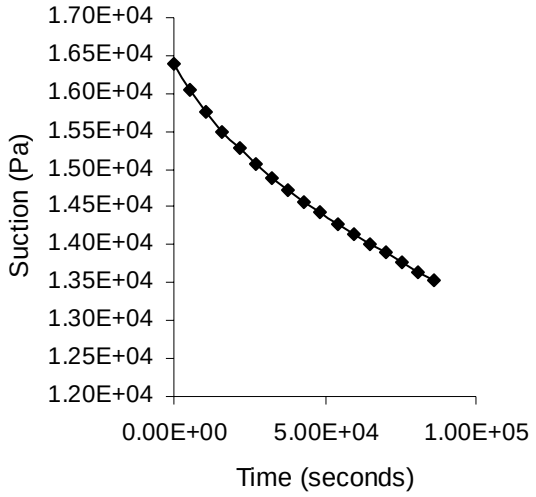

(a) At node 38

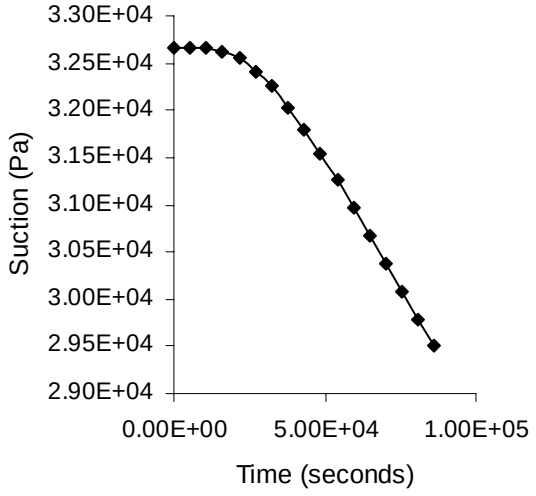

b) At node 73

Figure 4.3: Time histories of matric suction

To analyze the effects of rainfall infiltration in vertical profiles, nodes 90, 75, 60 and nodes 140, 125 and 110 are carefully chosen. The change of matric suction versus time for these nodes are shown in Figure 4.4.

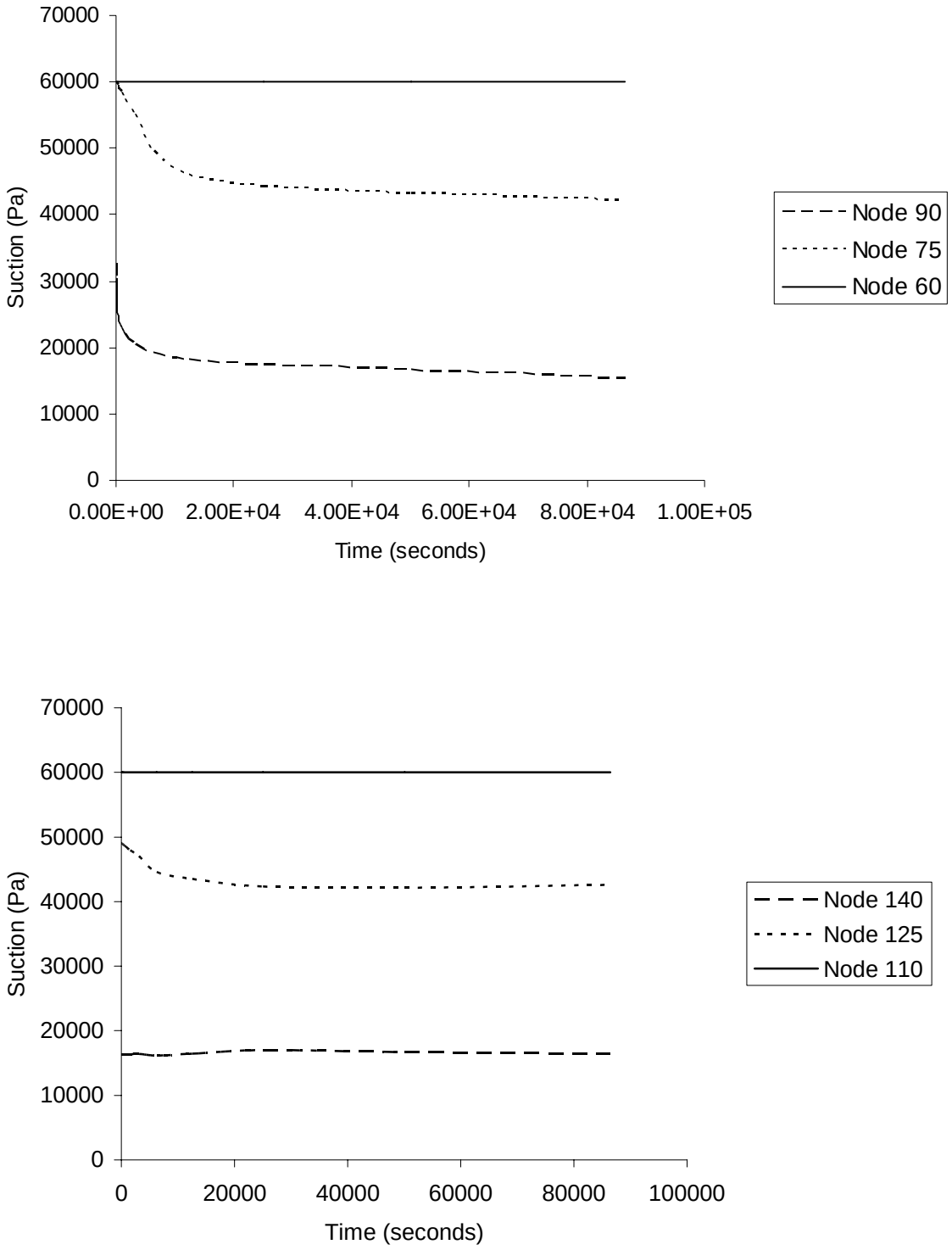

Figure 4.4: Time histories of matric suction at two different vertical profiles

The time histories of net mean stress are given in Figure 4.5. The increase in net mean stress with time as presented in Figure 4.5 (a) and 4.5 (b) can be attributed to the increase in unit weight of soil due to increase of moisture content. This should stabilize as the soil becomes saturated at which the net stress becomes the effective stress as described by Terzaghi's effective stress equation. The rate of change of effective stress depends on the increase in unit weight and pore water pressure.

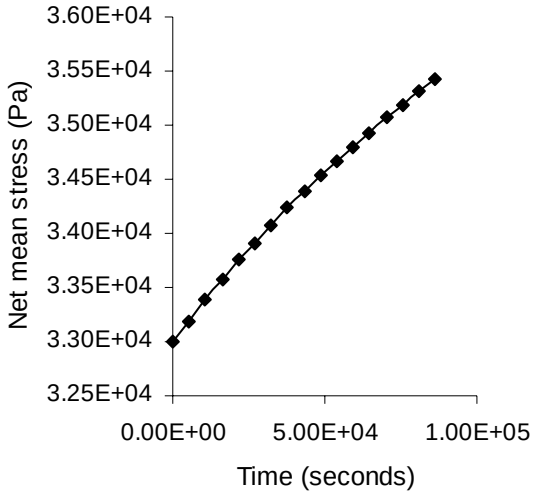

(a) At node 38

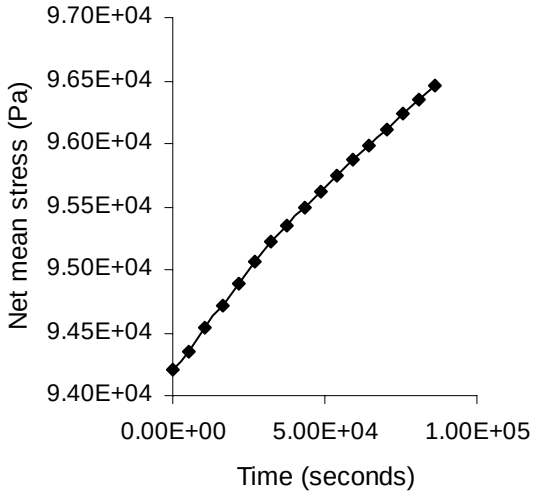

(b) At node 73

Figure 4.5: Time histories of net mean stress

Figure 4.6(a), 4.6(b) and 4.6(c), gives pressure of water contours at 6, 12 and 18 hours respectively. It is observed that the rainfall infiltration has little effect on the ground water table, but has a dramatic effect on the pressure of water above the ground water table in the unsaturated zone.

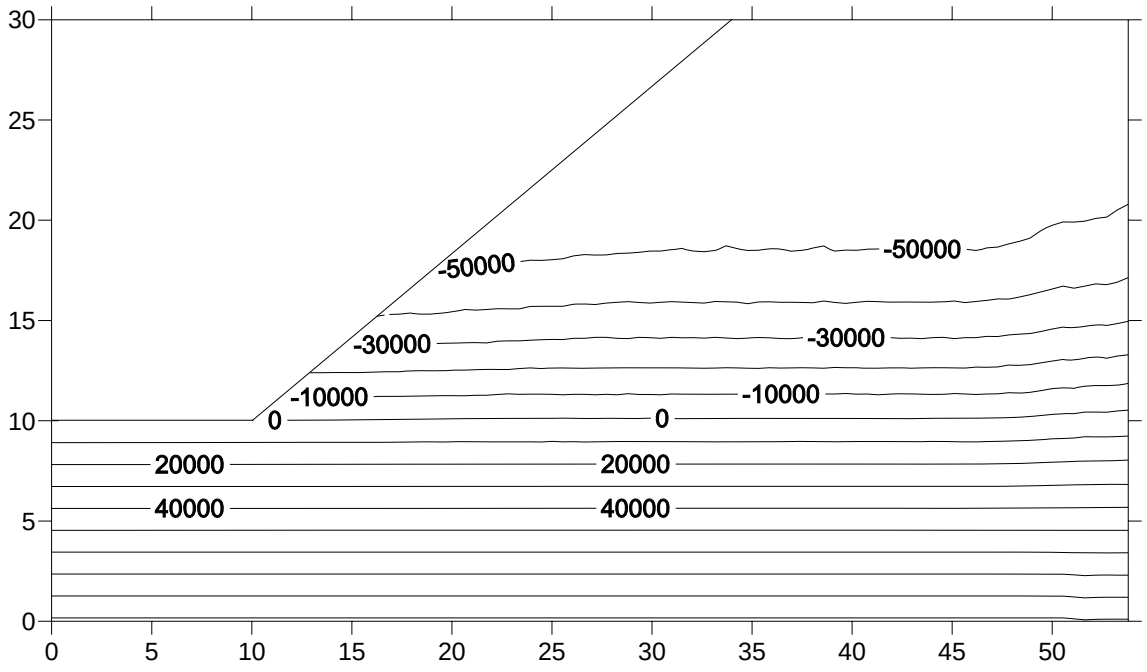

Figure 4.6 (a): Pressure of water contour at 6 hours

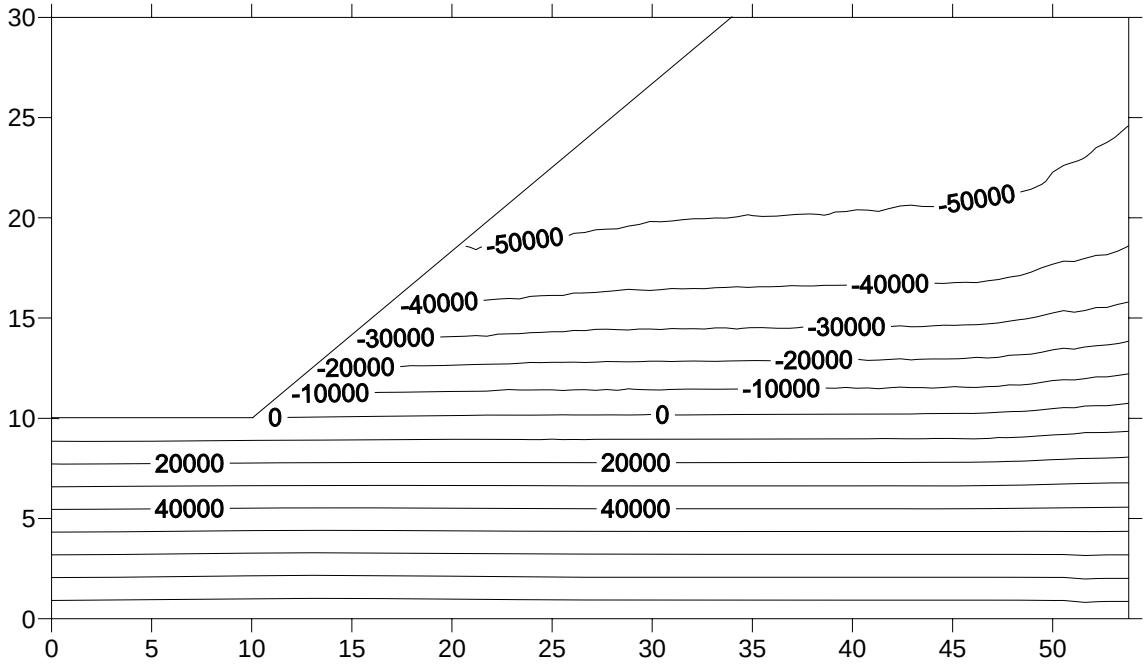

Figure 4.6 (b): Pressure of water contour at 12 hours

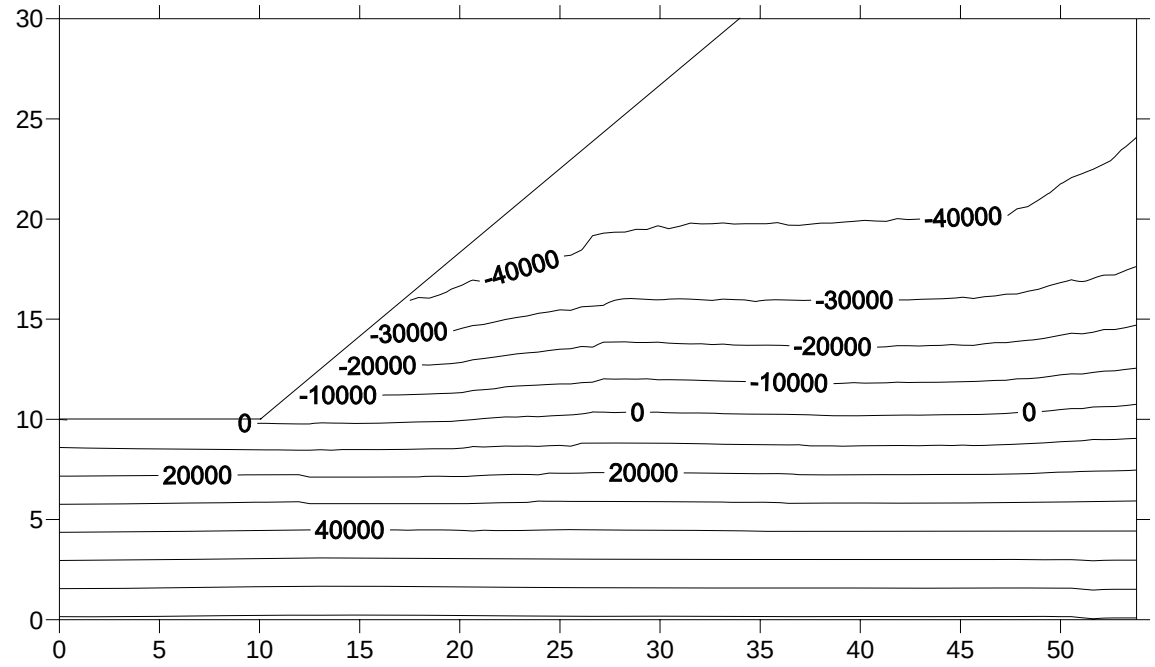

Figure 4.6 (c): Pressure of water contour at 18 hours

Induced deformations at 6, 12, and 18 hours after consistent rainfall is presented in Figure 4.7(a), 4.7(b), and 4.7(c) as vector diagrams.

As expected the arrowheads of the diagram points to the toe of the slope professing an impending circular slope failure. As the time increases, it can be seen that the nodes further away to the toe undergo larger displacements, and confirms to the theory that if rainfall continues for a long period of time, a deeper failure will occur. As expected, it can be seen that the soil in the saturated zone undergoes relatively smaller displacements compared to the soil in the unsaturated zone.

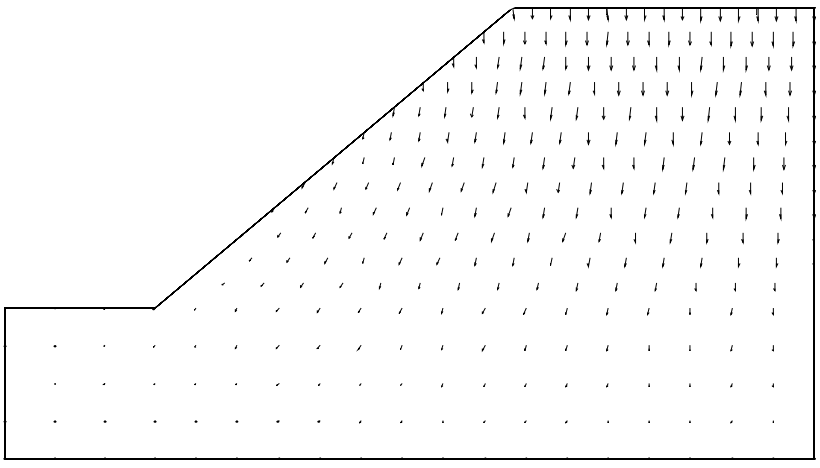

Figure 4.7 (a): Deformation vectors at 6 hours

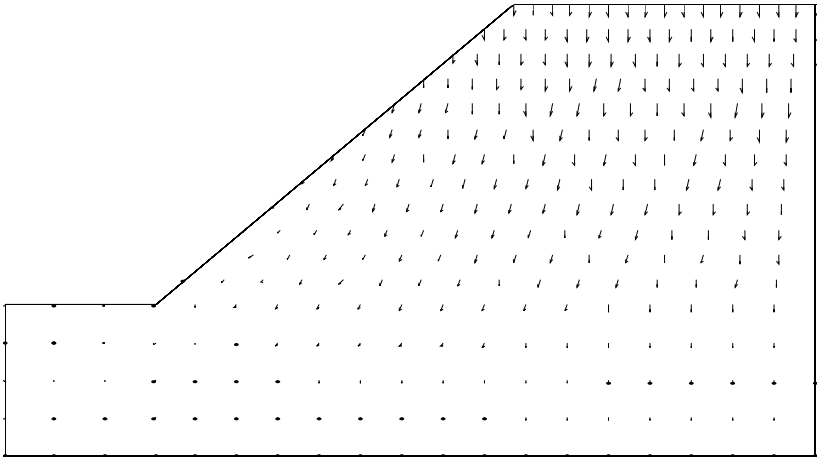

Figure 4.7 (b): Deformation vectors at 12 hours

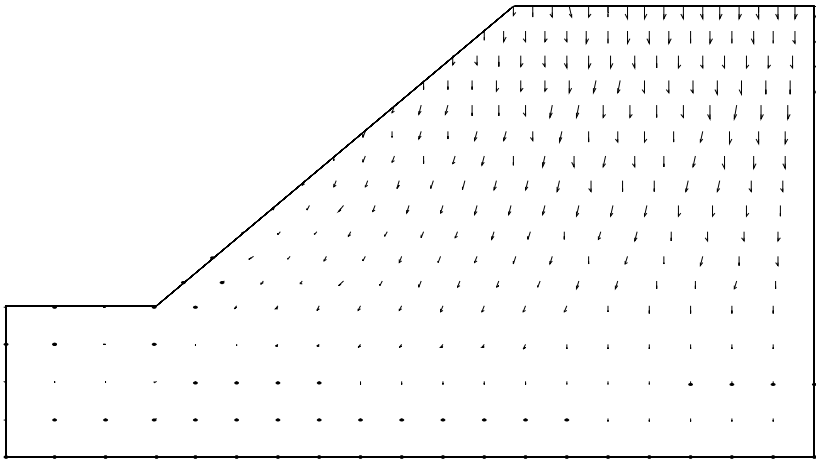

Figure 4.7 (c): Deformation vectors at 18 hours

Chapter 5

Conclusions

Numerical analysis plays an important role in the investigation of the behavior of partially saturated soils by highlighting aspects which are important in engineering practice and illustrating the effect of partial soil saturation on the behavior of geotechnical structures.

In this context, a finite element model was developed, and a numerical simulation was performed on a formulation taking into account the basic features of unsaturated soil behavior to a slope problem in residual soil subjected to rainfall. The response of the soil slope to rainfall perturbation was critically studied using time histories of matric suction, net mean stress and deformation.

However, the current study uses a non-linear elastic model based on Hooke's law. Therefore it is reasonable to continue the analyses only up to the stage where the slope failure does not occur, at which point the slope will start to exhibit plastic deformations. Further development is, therefore, required to describe the mechanical response of unsaturated soil with a nonlinear elasto-plastic formulation.

The current model is generic and can be easily modified to model a variety of soil problems by simply changing the mesh, boundary conditions, initial conditions, and the forcing function.

References

[1] Bishop, A. W. (1959). The principle of effective stress, *Publication 32*, Norwegian Geotechnical Institute, Oslo, Norway, 1–4.

[2] Bishop A. W., Blight G. E. (1963). Some aspects of effective stress in saturated and partly saturated soils. *Geotechnique 13,* No3, pp. 177-197.

[3] Fredlund, D.G., Rahardjo, H., 1995. *Soil Mechanics for Unsaturated Soils*. John Wiley and Sons, New York.

[4] Alonso E. E., Gens A., Josa A. (1990). A constitutive model for partially saturated soils. *Geotechnique 40*, No. 3, pp. 405-430.

[5] Alonso E. E., Vaunat J., Gens A. (2000). Modeling the mechanical behavior of expansive clays, *Engineering Geology*.

[6] Biot, M. A., and Willis, D. G. (1957). The elastic coefficients of the theory of consolidation, *J. Appl. Mech.,* 24, 594–601.

[7] Green, D. H., and Wang, H. F. (1990). Specific storage as a poroelastic coefficient, *Water Resour. Res.,* 26, 1631–1637.

[8] Cheng, A. H.-D. (1997). ‘‘Material coefficients of anisotropic poroelasticity, *Int. J. Rock Mech. Min. Sci.,* 34, 199–205.

[9] Desai, C. S., and Saxena, S. K. (1977) Consolidation analysis of layered anisotropic foundation, *Int. J. Numer. Analyst. Meth. Geomech.,* 1, 5–23.

[10] Behrouz Gatmiri, Ehsan Jabbari (2005) Time-domain Green’ s functions for unsaturated soils. Part I: Two-dimensional solution. *International Journal of Solids and Structures* 42:5971–5990.

[11] Jacquard C (1988) *Etude experimentale d’une barriere capillaire avec un modele de laboratoire*. PhD Thesis, CGI, Ecole Mines Paris. 165 pp

[12] Brun P (1989) *Cinetique d’infiltration au sein d’une couche d’argile compaclee. Etude experimentale el numerique*. PhD Thesis, ENSMP, Paris. 219pp.

[13] Lu, N., and Likos, W. J. (2004). *Unsaturated soil mechanics*, Wiley, N.J.

[14] Asian Disaster Preparedness Center (ADPC), 2006. Rapid assessment: Flashflood and landslide disaster in the provinces of Uttaradit and Sukhothai northern Thailand. Urban Disaster Management, ADPC, Thailand.

[15] Alonso, E.E., Battle, F., Gens, A., Lloret, A.,1988. Consolidation analysis of partially saturated soils - application to earth dam construction. In: Proceedings of the International Conference on Num. Meth. Geomechnics. Innsbruck. pp 1303–1308.

[16] Duncan, J.M., 1996. State of the art: Limit equilibrium and finite-element analysis of slopes. Journal of Geotechnical Engineering 122(7):577–596.

[17] Gasmo, J.M., Rahardjo, H., Leong, E.C., 2000. Infiltration effects on stability of a residual soil slope. Computer and Geotechnics 26:145–165.

[18] Gatmiri, B., Jabbari, E., 2005. Time-domain Green's functions for unsaturated soils. Part I: Two-dimensional solution. International journal of solids and structures 42 (23):5971–5990.

[19] Green, D.H., Wang, H.F., 1990. Specific storage as a poroelastic coefficient. Journal of Applied Mechanics 26:1631–1637.

[20] Jacquard, C., 1988. Etude experimentale dune barriere capillaire avec un modele de laboratoire. PhD Thesis, CGI, Ecole Mines Paris. 165 pp.

[21] Krahn, J., Fredlund, D.G., Klassen, G.M., 1989. Effect of soil suction on slope stability at notch hill. Canadian Geotechnical Journal 26:269–278.

[22] Lewis, R.W., Schrefler, B.A., 1989. Finite element method in the deformation and consolidation of porous media. Wiley, Chichester

[23] Neaupane, K.M., Piantanakulchai, M., 2006. Analytic Network Process Model for Landslide Hazard Zonation. Engineering Geology 85:281–294.

[24] Neaupane K.M., Yamabe, T., 2001. A fully coupled thermo-hydro-mechanical nonlinear model for a frozen medium. Computer and Geotechnics 28:613–637.

[25] Ng, C.W.W., Shi, Q., 1998. A numerical investigation of the stability of unsaturated soil slopes subjected to transient Seepage. Computer and Geotechnics 22:1–28.

[26] Singh, V.K, Lukmuang, M., Glawe, U., 2003. Observations on Landslides Resulting from Extreme Rainfalls in the NE of Thailand (Phu Rua District, Loei Province.,. In:Int. Conf. Slope Eng. University of Hongkong, Hongkong Vol. 1 pp 203–207.

[27] Tsaparas, I., Rahardjo, H., Toll, D.G., Leong, E.C., 2002. Controlling parameters for rainfall-induced landslides. Computer and Geotechnics 29:1–27.